

Lossless anomalous dispersion and an inversionless gain doublet via dressed interacting ground states (DIGS)

James Owen Weatherall^{1,2,3} and Christopher P. Search¹

¹*Department of Physics and Engineering Physics, Stevens Institute of Technology,
Castle Point on Hudson, Hoboken, NJ 07030, USA*

²*Department of Mathematical Sciences, Stevens Institute of Technology,
Castle Point on Hudson, Hoboken, NJ 07030, USA*

³*Department of Logic and Philosophy of Science, UC Irvine,
3151 Social Science Plaza A, Irvine, CA 92697, USA*

(Dated: November 17, 2018)

Transparent media exhibiting anomalous dispersion have been of considerable interest since Wang, Kuzmich, and Dogariu [Nature **406**, 277 (2000)] first observed light propagate with superluminal and negative group velocities without absorption. Here, we propose an atomic model exhibiting these properties, based on a generalization of amplification without inversion in a five-level DIGS system. The system consists of a Λ atom prepared as in standard electromagnetically induced transparency (EIT), with two additional metastable ground states coupled to the Λ atom ground states by two RF/microwave fields. We consider two configurations by which population is incoherently pumped into the ground states of the atom. Under appropriate circumstances, we predict a pair of new gain lines with tunable width, separation, and height. Between these lines, absorption vanishes but dispersion is large and anomalous. The system described here is a significant improvement over other proposals in the anomalous dispersion literature in that it permits additional coherent control over the spectral properties of the anomalous region, including a possible 10^4 -fold increase over the group delay observed by Wang, Kuzmich, and Dogariu.

I. INTRODUCTION

It has long been predicted that under certain conditions, optical media exhibit anomalous dispersion (ie. the index of refraction increases with increasing wavelength) [1]. In these cases, the group velocity of a pulse of light with appropriate frequency can be larger than the speed of light in a vacuum or negative [2]. Negative group velocity implies that a smoothly varying pulse of light will appear to exit the dispersive medium before it enters [3]. This is possible because different spectral components of the pulse interfere strongly in the dispersive region and transform the leading edge of the pulse into an image of the pulse's peak. Thus it is only with regard to the overall profile of the pulse that superluminal propagation appears to occur; anomalous dispersion does not permit superluminal signalling and causality is not violated [4, 5, 6, 7].

In 2000, Wang, Kuzmich, and Dogariu were first to observe light propagating with negative group velocities in a region of low absorption and minimal reshaping in a Rb vapor cell [8, 9]. Their experiment was based on a system proposed by Steinberg and Chiao [10], in which a Λ atom with the excited state coupled to one ground state by two far-detuned pump lasers is probed by a weak beam near the transition between the excited state and the second ground state. With appropriate initial conditions, this configuration leads to two narrowly spaced Raman gain lines in the probe's spectrum, with a region of anomalous dispersion but low absorption between them. In 2003, Bigelow et al. reported superluminal (and subluminal) group velocities in a room temperature solid (specifically, an alexandrite crystal) [11, 12]. That same

year, the claim that causality is maintained in cases of superluminal group velocities was supported experimentally by Stenner et al., who showed that the detection of a non-analytic point in an incident wave (representing new information) on the far side of a region of anomalous dispersion took at least as long as in the vacuum case [13]. It is now well established that superluminal and negative group velocities are possible in otherwise transparent and non-interfering media without violating relativity or causality.

In the decade since these first experiments, systems exhibiting anomalous dispersion have received considerable attention in the literature, among theorists and experimentalists. Some of these studies followed up on early predictions that strongly-driven two level atoms [14, 15, 16, 17, 18] and degenerate three level atoms [19, 20] can also exhibit regions of large anomalous dispersion but low absorption (for a comparative study of systems of these sorts and additional references, see [21]). Others have involved coupling the excited states of a V atom [22] or the ground states of a Λ atom [23] and then using the coupling field to coherently control the sign of the dispersion, while others still have employed a magnetic field to induce a Zeeman splitting, to similar effect [24, 25]. Many of these subsequent studies have involved coherent modification of the Raman gain process proposed by Steinberg and Chiao by introducing a second excited state [26, 27, 28, 29, 30, 31, 32] or a second excited state and a third ground state [33].

In the current contribution, we present a novel proposal for producing a narrow, closely-spaced gain doublet with an intermediate window of anomalous dispersion, using dressed interacting ground states (DIGS).

DIGS systems [34, 35] are a generalization of the double dark resonances (sometimes called interacting dark resonances) introduced by Lukin et al. [36]. Double dark resonances occur when one ground state of a Λ atom is strongly coupled to the excited state (as in standard EIT), and also coupled to a third ground state via an RF/microwave field. The result is a standard EIT absorption spectrum, with a new absorption peak located at zero probe detuning. New absorption nulls appear to either side of this peak. These systems have been studied extensively and observed experimentally [36, 37, 38, 39, 40, 41, 42]. DIGS systems include a fourth ground state (to produce a five-level atom) coupled to the second Λ ground state by a second RF/microwave field. This additional coupling has been predicted to split the double dark resonance absorption peak into two symmetric peaks located within the transparency window [34]. These peaks have widths and locations that are tunable by varying the RF/microwave Rabi frequencies, leading to additional control over the optical response of an atomic system.

Here, we modify the model presented in [34] by introducing pumping terms. The pumping transforms the lines we describe in the earlier paper into the pair of gain lines. The system studied here has several benefits over previously considered examples exhibiting anomalous dispersion. For one, even in the cases where the Raman gain lines were shown to have tunable heights and signs, there was no independent control over their widths. Moreover, here the locations of the gain lines vary with the field strengths, not frequency or phase, and so they are easier to tune than a Raman system, where the location of the peaks depends on the laser frequencies. The lines we predict have tunable locations, widths, and heights (allowing the smooth change of the sign of both the absorption coefficient and dispersion), and so the current system permits a very narrow window with ultrahigh anomalous dispersion, or alternatively, a maximally broad window throughout which anomalous dispersion is present. We predict that in a cold Rb gas prepared in analogy to the experiment in Ref. [43], one could observe a negative group velocity index two orders of magnitude larger than the largest yet observed of -14000 [44], and four orders of magnitude larger than the group velocity index reported by Wang, Kuzmich, and Dogariu [8].

Since the gain described here is generated without appreciable population accumulating in the excited state, the phenomenon we predict can be thought of as a generalized example of amplification without inversion (AWI), which is often also referred to as lasing without inversion [45, 46]. Unlike standard AWI [47, 48, 49], however, the current system requires only incoherent pumping to exhibit gain, as opposed to coherent pumping. We derive analytic results to describe the optical response as a function of the incoherent pumping rate(s) in both open and closed pumping configurations. These analytic results are a central feature of the current paper, as previous presen-

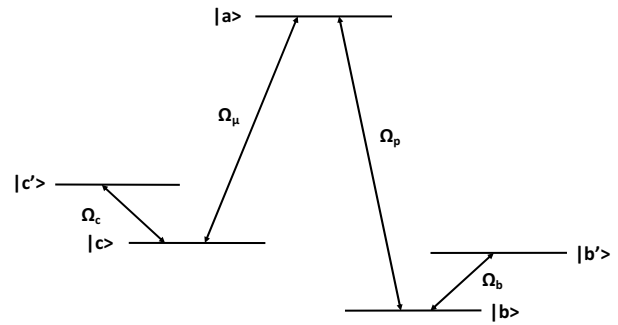


FIG. 1: Our five level model. An excited state $|a\rangle$ is coupled to two lower energy state doublets, $\{|b\rangle, |b'\rangle\}$ and $\{|c\rangle, |c'\rangle\}$. Ω_μ is the Rabi frequency of a strong control beam coupling $|a\rangle$ and $|c\rangle$; Ω_b and Ω_c are the Rabi frequencies of two RF/microwave fields coupling the members of each of the doublets. We study the propagation of a weak probe beam with Rabi frequency $\Omega_p \ll \Omega_c, \Omega_b, \Omega_\mu$ near resonance with the $|a\rangle \leftrightarrow |b\rangle$ transition. The specifics of the decay and pumping schemes will be treated in sections III A and III B.

tations of related systems (eg. double dark state systems with pumping) present exclusively numerical solutions.

The remainder of the paper will be organized as follows. In section II, we will review the base model that we consider in this paper. For further details on the model, see [34]. In section III we will solve the master equations for both open and closed pumping configurations. In section IV, we will derive the linear susceptibility for the probe beam. Here, we will present an explanation and analysis of the gain lines and the anomalous dispersion mentioned above. Section V will treat Doppler broadening in the DIGS system. Finally, in section VI we will offer some conclusions, including a discussion of possible experimental realizations.

II. MODEL PRELIMINARIES

Our base system is a five-level atom (see Fig. 1) in which two sets of ground states, $\{|b\rangle, |b'\rangle\}$ and $\{|c\rangle, |c'\rangle\}$, interact with a single excited state, $|a\rangle$. Transitions between each of the ground state doublets are assumed to be dipole forbidden; the members of the hyperfine ground state doublets, meanwhile, are coupled via RF/microwave fields (in what follows, we will refer to these as RF fields for simplicity) of frequencies ω_b and ω_c . These fields have Rabi frequencies Ω_b and Ω_c . One of the states in the $\{|c\rangle, |c'\rangle\}$ manifold (without loss of generality, $|c\rangle$) is strongly coupled to $|a\rangle$ by a field with Rabi frequency Ω_μ . We study the optical response of a field near resonance with the $|b\rangle \leftrightarrow |a\rangle$ transition, with Rabi frequency Ω_p . We describe this system via the Hamilto-

nian

$$\begin{aligned} \tilde{\mathcal{H}} = & \frac{\hbar}{2} (\omega_a |a\rangle\langle a| + (\omega_b + \nu_p) |b\rangle\langle b| + (\omega_{b'} + \nu_p - \nu_b) |b'\rangle\langle b'| \\ & + (\omega_c + \nu_\mu) |c\rangle\langle c| + (\omega_{c'} + \nu_\mu - \nu_c) |c'\rangle\langle c'| - \Omega_\mu |a\rangle\langle c| \\ & - \Omega_b |b'\rangle\langle b| - \Omega_c |c'\rangle\langle c| - \Omega_p |a\rangle\langle b|) + \text{h.c.} \end{aligned} \quad (1)$$

The $\tilde{\cdot}$ here indicates that we have written the Hamiltonian in a rotating basis defined to eliminate explicit time dependence. From the Hamiltonian we obtain the detunings for the control laser $\Delta_\mu = \omega_a - \omega_c - \nu_\mu$ and the RF fields, $\Delta_b = \omega_{b'} - \omega_b - \nu_b$ and $\Delta_c = \omega_{c'} - \omega_c - \nu_c$. Most importantly, the detuning of the probe laser from the $|b\rangle \leftrightarrow |a\rangle$ transition

$$\Delta_p = \omega_a - \omega_b - \nu_p \quad (2)$$

will be used to express the optical susceptibility of the probe field.

For further details on this base system (including an explicit definition of the rotating frame), see section II of [34]. The model considered there functions as the starting point for the current paper; it is essentially identical to the model described here, except for the pumping and decay schemes, representations of which will be discussed presently.

In what follows, we will be interested in the linear susceptibility expanded around the $|a\rangle \leftrightarrow |b\rangle$ transition, which can be written in terms of the corresponding density matrix element, $\tilde{\rho}_{ab}$. Since we are not yet considering any nonunitary contributions, the density matrix can be described by the von Neumann equation, $i\hbar d\rho/dt = [H, \rho]$. The equations of motion for the components of the density matrix follow immediately. They are given in Appendix A. In what follows, we will make reference to these in defining the models for each of the pumping configurations.

In the bare basis, we will find that to first order in Ω_p/Ω_μ (with assumptions that we describe below) $\tilde{\rho}_{ab}$ depends on the solutions to six linked differential equations, which in general cannot be solved analytically. However, under the rotation defined in [34], in which we diagonalize the $\{|b\rangle, |b'\rangle\}$ and $\{|c\rangle, |c'\rangle\}$ subspaces of the Hamiltonian, these six linked equations decouple into two systems of three equations each. The details of the change of basis are given in appendices B and C. We will distinguish the diagonalized states by using capital letters, $\{|b\rangle, |b'\rangle\} \rightarrow \{|B\rangle, |B'\rangle\}$ and $\{|c\rangle, |c'\rangle\} \rightarrow \{|C\rangle, |C'\rangle\}$. The transformation for each of the subspaces individually is of the same form as the dressed states of a two level atom.

III. SOLUTIONS TO THE MASTER EQUATION

Here we present and solve the Linblad equation for the evolution of the density matrix in both open (section III A) and closed (section III B) pumping configurations. In each case, we are focused on finding a linear solution

for $\tilde{\rho}_{ab}$ from which we can derive the linear susceptibility for the probe beam in section IV.

A. Open pumping configuration

As mentioned in the introduction, the amplification presented here does not require population inversion. It does require, however, that population be distributed between the ground states—specifically in $\{|b\rangle, |b'\rangle\}$ and $|c'\rangle$. The details of this requirement are most clearly manifest when we populate these states directly, via pumping from unspecified external states. This is the case we consider in the current section: the ground states $|b\rangle$ and $|c'\rangle$ are pumped from external levels; likewise, decay occurs to external levels. Note that we would obtain essentially the same results if we added additional pumping to the levels $|b'\rangle$ and $|c\rangle$ since Ω_b distributes the population between $|b\rangle$ and $|b'\rangle$ while in the limit we are interested in ($\Omega_c \ll \Omega_\mu$), any population in $|c\rangle$ is optically pumped into $|c'\rangle$.

To model pumping from and decay to external states, we modify Eqs. A1 by including terms to model direct incoherent pumping to $|b\rangle$ and $|c'\rangle$, at rates r_b and $r_{c'}$ respectively.

$$i \frac{\partial \tilde{\rho}_{jj}}{\partial t} \sim i r_j \quad j = b, c'$$

Relaxation terms are modeled by,

$$\begin{aligned} i \frac{\partial \tilde{\rho}_{jj}}{\partial t} & \sim -i \gamma_j \rho_{jj} \\ i \frac{\partial \tilde{\rho}_{jk}}{\partial t} & \sim -i \gamma_{jk} \rho_{jk} \quad j \neq k \end{aligned}$$

where γ_j is the decay from state $|j\rangle$ and $\gamma_{jk} = \frac{1}{2}(\gamma_j + \gamma_k) + \gamma_{jk}^{\text{ph}}$ is the full off-diagonal relaxation term.

Our strategy in what follows will be to assume that $\Omega_p \ll \Omega_b, \Omega_c, r_b, r_{c'} \ll \Omega_\mu$, and then use two applications of perturbation theory. First, we work at zeroth order in Ω_p/Ω_μ , which essentially decouples the $\{|b\rangle, |b'\rangle\}$ manifold from $|a\rangle, |c\rangle$, and $|c'\rangle$. The $\{|b\rangle, |b'\rangle\}$ subspace can be solved exactly at this order. The $\{|a\rangle, |c\rangle, |c'\rangle\}$ subspace is more complicated. However, under the approximations already described $\tilde{\rho}_{c'c'}$ varies slowly relative to the other terms of the density matrix in this subspace, and so we can assume the other terms will follow it adiabatically. Then we can solve for the other terms to first order in Ω_c/Ω_μ as a function of the steady state population of $|c'\rangle$, $\tilde{\rho}_{c'c'}^{\text{st}}$, and use these first order solutions to find a self-consistent solution for $\tilde{\rho}_{c'c'}^{\text{st}}$ valid to order $(\Omega_c/\Omega_\mu)^2$. Finally, we will move to the dressed basis introduced in section II and defined in appendix B and solve for $\tilde{\rho}_{ab}$ to first order in Ω_p/Ω_μ using the zeroth order (in Ω_p/Ω_μ) solutions as source terms.

We assume that the control and RF fields are on resonance, $\Delta_\mu = \Delta_b = \Delta_c = 0$. (A full general solution for the susceptibility with arbitrary nonzero detunings is included in appendix D. The derivation is identical to the

current case.) Then, to zeroth order in Ω_p/Ω_μ , the equations of motion for the $\{|b\rangle, |b'\rangle\}$ manifold can be written as

$$i\frac{\partial\tilde{\rho}_{bb}}{\partial t} = ir_b - i\gamma_b\tilde{\rho}_{bb} + \frac{\Omega_b}{2}(\tilde{\rho}_{bb'} - \tilde{\rho}_{b'b}) \quad (3a)$$

$$i\frac{\partial\tilde{\rho}_{b'b'}}{\partial t} = -i\gamma_{b'}\tilde{\rho}_{b'b'} - \frac{\Omega_b}{2}(\tilde{\rho}_{bb'} - \tilde{\rho}_{b'b}) \quad (3b)$$

$$i\frac{\partial\tilde{\rho}_{bb'}}{\partial t} = -\gamma_{bb'}\tilde{\rho}_{bb'} + \frac{\Omega_b}{2}(\tilde{\rho}_{bb} - \tilde{\rho}_{b'b'}) \quad (3c)$$

These can be solved by writing them in the form $\frac{\partial X}{\partial t} = -MX + A$, which has a steady state solution of $X = M^{-1}A$. We find

$$\tilde{\rho}_{bb}^{\text{st}} = \frac{r_b(2\gamma_{b'}\gamma_{bb'} + \Omega_b^2)}{2\gamma_b\gamma_{b'}\gamma_{bb'} + (\gamma_b + \gamma_{b'})\Omega_b^2} \quad (4a)$$

$$\tilde{\rho}_{b'b'}^{\text{st}} = \frac{r_b\Omega_b^2}{2\gamma_b\gamma_{b'}\gamma_{bb'} + (\gamma_b + \gamma_{b'})\Omega_b^2} \quad (4b)$$

$$\tilde{\rho}_{bb'}^{\text{st}} = (\tilde{\rho}_{b'b'}^{\text{st}})^* = \frac{-ir_b\gamma_{b'}\Omega_b}{2\gamma_b\gamma_{b'}\gamma_{bb'} + (\gamma_b + \gamma_{b'})\Omega_b^2}. \quad (4c)$$

To zeroth order in Ω_p/Ω_μ , our equations of motion for the $\{|a\rangle, |c\rangle, |c'\rangle\}$ subspace are, first for the diagonal terms,

$$i\frac{\partial\rho_{aa}}{\partial t} = -i\gamma_a\rho_{aa} - \frac{\Omega_\mu}{2}(\rho_{ca} - \rho_{ac}) \quad (5a)$$

$$i\frac{\partial\rho_{cc}}{\partial t} = -i\gamma_c\rho_{cc} + \frac{\Omega_\mu}{2}(\rho_{ca} - \rho_{ac}) + \frac{\Omega_c}{2}(\rho_{cc'} - \rho_{c'c}) \quad (5b)$$

$$i\frac{\partial\rho_{c'c'}}{\partial t} = ir_{c'} - i\gamma_{c'}\rho_{c'c'} - \frac{\Omega_c}{2}(\rho_{cc'} - \rho_{c'c}) \quad (5c)$$

and for the off-diagonal terms,

$$i\frac{\partial\tilde{\rho}_{ca}}{\partial t} = -i\gamma_{ca}\tilde{\rho}_{ca} + \frac{\Omega_\mu}{2}(\tilde{\rho}_{cc} - \tilde{\rho}_{aa}) - \frac{\Omega_c}{2}\tilde{\rho}_{c'a} \quad (5d)$$

$$i\frac{\partial\tilde{\rho}_{c'a}}{\partial t} = -i\gamma_{c'a}\tilde{\rho}_{c'a} + \frac{\Omega_\mu}{2}\tilde{\rho}_{c'c} - \frac{\Omega_c}{2}\tilde{\rho}_{ca} \quad (5e)$$

$$i\frac{\partial\tilde{\rho}_{c'c}}{\partial t} = -i\gamma_{c'c}\tilde{\rho}_{c'c} + \frac{\Omega_\mu}{2}\tilde{\rho}_{c'a} + \frac{\Omega_c}{2}(\tilde{\rho}_{c'c'} - \tilde{\rho}_{cc}) \quad (5f)$$

We assume that $\Omega_\mu, \gamma_a \gg \Omega_c, r_{c'}, \gamma_c, \gamma_{c'}$. With these assumptions, it is clear that all of the equations of motion, except the one governing $\tilde{\rho}_{c'c'}$, are dominated by the terms proportional to Ω_μ and γ_a . This is our justification for the claim that $\tilde{\rho}_{c'c'}$ varies slowly relative to the other terms in this subspace, and that therefore $\tilde{\rho}_{c'c'}$ can be treated as a constant with respect to the other equations of motion.

To zeroth order in Ω_c/Ω_μ , we have two decoupled systems of homogeneous equations. The steady state occurs only when $\tilde{\rho}_{c'a}^{(0)} = \tilde{\rho}_{c'c}^{(0)} = \tilde{\rho}_{aa}^{(0)} = \tilde{\rho}_{cc}^{(0)} = \tilde{\rho}_{ca}^{(0)} = 0$. Physically, this makes sense, since the system is non-conservative and there is no external pumping to these levels/coherences. To first order in Ω_c/Ω_μ , $\tilde{\rho}_{aa}^{(1)} = \tilde{\rho}_{cc}^{(1)} =$

$\tilde{\rho}_{ca}^{(1)} = 0$ again, since the equations of motion are unchanged at this order. The second system, however, now leads to nonzero steady state values. These are

$$\tilde{\rho}_{c'a}^{(1)} = \tilde{\rho}_{c'c'}^{\text{st}} \frac{-\Omega_c\Omega_\mu}{4\gamma_{c'c}\gamma_{c'a} + \Omega_\mu^2} \quad (6)$$

$$\tilde{\rho}_{c'c}^{(1)} = \tilde{\rho}_{c'c'}^{\text{st}} \frac{-2i\gamma_{c'a}\Omega_c}{4\gamma_{c'c}\gamma_{c'a} + \Omega_\mu^2} \quad (7)$$

This linear solution is sufficient to reproduce the effect that we are interested in. Taking the first order solutions as the steady states, we can solve self-consistently for $\tilde{\rho}_{c'c'}^{\text{st}}$. We find

$$\tilde{\rho}_{c'c'}^{\text{st}} = \frac{r_{c'}}{\left(\frac{2\Omega_c^2\gamma_{c'a}}{4\gamma_{c'c}\gamma_{c'a} + \Omega_\mu^2} + \gamma_{c'}\right)}. \quad (8)$$

We are now very nearly in a position to solve for $\tilde{\rho}_{ab}$ to first order in Ω_p/Ω_μ . We move now to the dressed basis defined in appendix B. The assumptions already stated, $\Delta_b = \Delta_c = 0$, imply that $\Omega_b^{\text{eff}} = \Omega_b$, $\Omega_c^{\text{eff}} = \Omega_c$, and $\theta_b = \theta_c = \pi/4$ (see appendix B for definitions of these terms). In order to handle decay analytically, we assume that $\gamma_{ab} = \gamma_{ab'}$. This is reasonable, supposing both expressions will be dominated by $\gamma_a \gg \gamma_b, \gamma_{b'}, \gamma_{a,b}^{\text{ph}}, \gamma_{a,b'}^{\text{ph}}$. Moreover, we assume that $\gamma_b \approx \gamma_{b'}$, $\gamma_{bc}^{\text{ph}} \approx \gamma_{b'c}^{\text{ph}}$, and $\gamma_{bc'}^{\text{ph}} \approx \gamma_{b'c'}^{\text{ph}}$, so that we can take $\gamma_{cb} \approx \gamma_{cb'} = \gamma_C$ and $\gamma_{c'b} \approx \gamma_{c'b'} = \gamma_{C'}$. In Appendix C we give full expressions for the decay and dephasing of the relevant density matrix components in the dressed basis in terms of the γ_{ab} , γ_C , and $\gamma_{C'}$. These approximations may seem slightly arbitrary, but they permit both enough simplification to solve the problem entirely, and yet contain enough nuance for an adequate analysis of the effects of decoherence on the phenomena we predict. Finally, we assume that $\gamma_{cc'}, \gamma_{bb'}, \gamma_C, \gamma_{C'} \ll \Omega_\mu$, as would occur, say, in a cold atomic gas, or in a hot gas with a buffer gas present.

We already have that $\tilde{\rho}_{aa}^{(1)} = 0$; moreover, under these new assumptions, $\tilde{\rho}_{c'a}^{(1)} = -\frac{\Omega_c}{\Omega_\mu}\tilde{\rho}_{c'c'}$, which gives that (see appendix B) $\tilde{\rho}_{c'a} = \tilde{\rho}_{Ca} = -\frac{\sqrt{2}}{2}\frac{\Omega_c}{\Omega_\mu}\tilde{\rho}_{c'c'}^{\text{st}}$. Meanwhile, $\tilde{\rho}_{bb} \approx \tilde{\rho}_{b'b'} \approx \frac{r_b}{\gamma_b + \gamma_{b'}}$ and $\tilde{\rho}_{bb'} \approx \frac{-ir_b\gamma_{b'}}{(\gamma_b + \gamma_{b'})\Omega_b}$. The diagonalization leaves these invariant, and so $\tilde{\rho}_{BB} \approx \tilde{\rho}_{B'B'} \approx \frac{r_b}{\gamma_b + \gamma_{b'}}$ and $\tilde{\rho}_{BB'} = (\tilde{\rho}_{B'B})^* \approx \frac{-ir_b\gamma_{b'}}{(\gamma_b + \gamma_{b'})\Omega_b}$. Taking these together, we find steady state solutions

$$\tilde{\rho}_{aB} = \frac{\sqrt{2}\Omega_p}{2Z_+} (\mathfrak{P}_B (2i\gamma_C - 2\Delta_p - \Omega_b) \times (2i\gamma_{C'} - 2\Delta_p - \Omega_b) + \Omega_c^2 (\tilde{\rho}_{c'c'}^{\text{st}} - \mathfrak{P}_B)) \quad (9)$$

and

$$\tilde{\rho}_{aB'} = -\frac{\sqrt{2}\Omega_p}{2Z_-} (\mathfrak{P}_B (2i\gamma_C - 2\Delta_p + \Omega_b) \times (2i\gamma_{C'} - 2\Delta_p + \Omega_b) + \Omega_c^2 (\tilde{\rho}_{c'c'}^{\text{st}} - \mathfrak{P}_B)) \quad (10)$$

where

$$Z_{\pm} = \Omega_{\mu}^2(2i\gamma_{c'} - 2\Delta_p \mp \Omega_b) - (2i\gamma_{ab} - 2\Delta_p \mp \Omega_b) \times \left((i\gamma_c + i\gamma_{c'} - 2\Delta_p \mp \Omega_b)^2 - \Omega_c^2 \right) \quad (11)$$

and where we have defined $\mathfrak{P}_B = \frac{r_b(\Omega_b - i\gamma_b)}{(\gamma_b + \gamma_{b'})\Omega_b}$ (for a general definition of \mathfrak{P}_B , see appendix D). Meanwhile, to be consistent with the other approximations made thus far we should note that $\tilde{\rho}_{c'c'}^{\text{st}}$ simplifies to

$$\tilde{\rho}_{c'c'}^{\text{st}} = \frac{r_{c'}\Omega_{\mu}^2}{2\gamma_{c'a}\Omega_c^2 + \gamma_{c'}\Omega_{\mu}^2}. \quad (12)$$

$\tilde{\rho}_{ab}$ can be found simply from Eqs. 9 and 10 via the relation $\tilde{\rho}_{ab} = \frac{\sqrt{2}}{2}(\tilde{\rho}_{aB} - \tilde{\rho}_{aB'})$.

B. Closed pumping configuration

We chose to present the open pumping configuration first because we feel it distills the important parts of the dynamics: as we will argue in section IV, population in two ground states, $|b\rangle$ and $|c'\rangle$ is sufficient to produce amplification of the probe beam. Thus the essential physics of the system is already present in Eqs. 9-11; some readers may prefer to skip directly to section IV now. However, the theoretical literature has tended to focus on closed systems. Moreover, in the open pumping configuration we pump $|c'\rangle$ directly, which begs the question of whether population will accumulate in $|c'\rangle$ in the steady state if it is not directly pumped there. For completeness, we will now present a more theoretically natural case, in which atoms are pumped directly from $|b\rangle$ to $|a\rangle$, from which they decay to $|b\rangle$, $|c\rangle$, and $|c'\rangle$. In the appropriate limit ($\Omega_b/\Delta_b \rightarrow 0$), the solution presented here is an analytic solution for the system described in, for instance, [40].

In the closed pumping case, atoms are pumped from $|b\rangle$ to $|a\rangle$, and decay is internal to our 5 level subspace. We assume that the ground states are stable for the purposes of the current calculation. $|a\rangle$ is assumed to decay only to $|b\rangle$, $|c\rangle$, and $|c'\rangle$, with branching ratios α_b , α_c , and $\alpha_{c'}$, respectively ($\alpha_b + \alpha_c + \alpha_{c'} = 1$). Since a nonzero value of $\tilde{\rho}_{c'c'}^{\text{st}}$ is necessary, it is crucial that $\alpha_{c'} \neq 0$. The base equations of motion, Eqs. A1, now have contributions

$$i\frac{\partial\tilde{\rho}_{aa}}{\partial t} \sim -i(\gamma_a + r)\tilde{\rho}_{aa} + ir\tilde{\rho}_{bb} \quad (13a)$$

$$i\frac{\partial\tilde{\rho}_{bb}}{\partial t} \sim i(\alpha_b\gamma_a + r)\tilde{\rho}_{aa} - ir\tilde{\rho}_{bb} \quad (13b)$$

$$i\frac{\partial\tilde{\rho}_{cc}}{\partial t} \sim i\alpha_c\gamma_a\tilde{\rho}_{aa} \quad (13c)$$

$$i\frac{\partial\tilde{\rho}_{c'c'}}{\partial t} \sim i\alpha_{c'}\gamma_a\tilde{\rho}_{aa}. \quad (13d)$$

The definitions of the off-diagonal relaxation rates are unchanged from the open pumping case, except that now $\gamma_b = \gamma_{b'} = \gamma_c = \gamma_{c'} = 0$.

Our strategy here will be the same as in the open pumping case. To zeroth order in Ω_p/Ω_{μ} , however, the two subsystems of the previous case no longer decouple. But we can again make an observation about the time scales in the problem that will permit some simplification. As before, we assume that $\Omega_{\mu} \gg \Omega_b, \Omega_c \gg r$; moreover, we take γ_a to be sufficiently less than Ω_{μ} for it to be the case that $\alpha_i\gamma_a$ is about an order of magnitude smaller than Ω_{μ} . These considerations allow us to assume that $\tilde{\rho}_{bb}$, $\tilde{\rho}_{b'b'}$, $\tilde{\rho}_{bb'}$, and $\tilde{\rho}_{c'c'}$ vary slowly relative to the other elements. We can thus assume that the rapidly varying ones follow these adiabatically. We again work perturbatively in Ω_p/Ω_{μ} , and solve for $\tilde{\rho}_{ac'}$ and $\tilde{\rho}_{c'c}$. Now, however, $\tilde{\rho}_{bb}$ and $\tilde{\rho}_{c'c'}$ depend on $\tilde{\rho}_{aa}$, and so to find a self-consistent second order solution for the slowly varying populations, we require a second order perturbative solution for the rapidly varying populations.

We again work under the assumption that the control and RF field detunings vanish. First, note that it is clear from inspection of the relevant equations of motion in Eqs. A1 that in the steady state, $\tilde{\rho}_{bb}^{\text{st}} = \tilde{\rho}_{b'b'}^{\text{st}}$. Meanwhile, we can solve for the rapidly varying terms perturbatively in Ω_c/Ω_{μ} . To zeroth order, we again find two sets of decoupled equations. The ones describing $\tilde{\rho}_{ac'}$ and $\tilde{\rho}_{cc'}$ are homogeneous and decoupled from the pumping at this order, and so they vanish. The second system now has an inhomogeneous term, $\tilde{\rho}_{bb}^{\text{st}}$. We find,

$$i\frac{\partial\tilde{\rho}_{aa}}{\partial t} = -i(\gamma_a + r)\tilde{\rho}_{aa} + ir\tilde{\rho}_{bb}^{\text{st}} - \frac{\Omega_{\mu}}{2}(\tilde{\rho}_{ca} - \tilde{\rho}_{ac}) \quad (14a)$$

$$i\frac{\partial\tilde{\rho}_{cc}}{\partial t} = i\alpha_c\gamma_a\tilde{\rho}_{aa} + \frac{\Omega_{\mu}}{2}(\tilde{\rho}_{ca} - \tilde{\rho}_{ac}) \quad (14b)$$

$$i\frac{\partial\tilde{\rho}_{ca}}{\partial t} = -i\gamma_{ca}\tilde{\rho}_{ca} + \frac{\Omega_{\mu}}{2}(\tilde{\rho}_{cc} - \tilde{\rho}_{aa}) \quad (14c)$$

These have a steady state solution of

$$\tilde{\rho}_{aa}^{(0)} = \tilde{\rho}_{bb} \left(\frac{r}{r + (1 - \alpha_c)\gamma_a} \right) \quad (15a)$$

$$\tilde{\rho}_{cc}^{(0)} = \tilde{\rho}_{bb} \left(\frac{r(2\alpha_c\gamma_a\gamma_{ca}^2 + \gamma_{ca}\Omega_{\mu}^2)}{(r + (1 - \alpha_c)\gamma_a)\gamma_{ca}\Omega_{\mu}^2} \right) \quad (15b)$$

$$\tilde{\rho}_{ca}^{(0)} = \tilde{\rho}_{bb} \left(\frac{r\alpha_c\gamma_a - i\gamma_{ca}}{(r + (1 - \alpha_c)\gamma_a)\gamma_{ca}\Omega_{\mu}} \right) \quad (15c)$$

To first order, the equations of motion for $\tilde{\rho}_{aa}$, $\tilde{\rho}_{cc}$, and $\tilde{\rho}_{ca}$ are unchanged, as the density matrix elements proportional to Ω_c are zero to zeroth order. The equations for $\tilde{\rho}_{c'a}$ and $\tilde{\rho}_{c'c}$, meanwhile, become

$$i\frac{\partial\tilde{\rho}_{c'a}}{\partial t} = -i\gamma_{c'a}\tilde{\rho}_{c'a} + \frac{\Omega_{\mu}}{2}\tilde{\rho}_{c'c} - \frac{\Omega_c}{2}\tilde{\rho}_{ca}^{(0)} \quad (16a)$$

$$i\frac{\partial\tilde{\rho}_{c'c}}{\partial t} = -i\gamma_{c'c}\tilde{\rho}_{c'c} + \frac{\Omega_{\mu}}{2}\tilde{\rho}_{c'a} + \frac{\Omega_c}{2}(\tilde{\rho}_{c'c'}^{\text{st}} - \tilde{\rho}_{cc}^{(0)}) \quad (16b)$$

These have a steady state solution of

$$\tilde{\rho}_{c'a}^{(1)} = \frac{\Omega_c(\Omega_\mu(\tilde{\rho}_{cc}^{(0)} - \tilde{\rho}_{c'c'}^{\text{st}}) + 2i\gamma_{c'c}\tilde{\rho}_{ca}^{(0)})}{4\gamma_{c'c}\gamma_{c'a} + \Omega_\mu^2} \quad (17a)$$

$$\tilde{\rho}_{c'c}^{(1)} = \frac{\Omega_c(2i\gamma_{c'a}(\tilde{\rho}_{cc}^{(0)} - \tilde{\rho}_{c'c'}^{\text{st}}) + \Omega_\mu\tilde{\rho}_{ca}^{(0)})}{4\gamma_{c'c}\gamma_{c'a} + \Omega_\mu^2} \quad (17b)$$

In the open pumping case, it was only necessary to solve for the coherences to first order in Ω_c/Ω_μ in order to find the second order population $\tilde{\rho}_{c'c}$. In contrast, to find a fully self-consistent second order solution for $\tilde{\rho}_{c'c}$ and $\tilde{\rho}_{bb}$ in the closed pumping case, we require a second order solution for $\tilde{\rho}_{aa}$ and $\tilde{\rho}_{cc}$. The equations of motion for $\tilde{\rho}_{c'a}$ and $\tilde{\rho}_{c'c}$ are unchanged at this order. The equations of motion for $\tilde{\rho}_{aa}$, $\tilde{\rho}_{cc}$, and $\tilde{\rho}_{ca}$ meanwhile are now

$$i\frac{\partial\tilde{\rho}_{aa}}{\partial t} = -i(\gamma_a + r)\tilde{\rho}_{aa} + ir\tilde{\rho}_{bb}^{\text{st}} - \frac{1}{2}\Omega_\mu(\tilde{\rho}_{ca} - \tilde{\rho}_{ac}) \quad (18a)$$

$$i\frac{\partial\tilde{\rho}_{cc}}{\partial t} = i\alpha_c\gamma_a\tilde{\rho}_{aa} - \frac{1}{2}\Omega_c(\tilde{\rho}_{c'c}^{(1)} - \tilde{\rho}_{cc'}^{(1)}) + \frac{1}{2}\Omega_\mu(\tilde{\rho}_{ca} - \tilde{\rho}_{ac}) \quad (18b)$$

$$i\frac{\partial\tilde{\rho}_{ca}}{\partial t} = -i\gamma_{ca}\tilde{\rho}_{ca} + \frac{1}{2}\Omega_\mu(\tilde{\rho}_{cc} - \tilde{\rho}_{aa}) - \frac{1}{2}\Omega_c\tilde{\rho}_{c'a}^{(1)} \quad (18c)$$

These are solved by

$$\tilde{\rho}_{aa}^{(2)} = \frac{2r\tilde{\rho}_{bb}^{\text{st}} + i(\tilde{\rho}_{c'c}^{(1)} - \tilde{\rho}_{cc'}^{(1)})\Omega_c}{2(r + (1 - \alpha_c)\gamma_a)} \quad (19a)$$

$$\begin{aligned} \tilde{\rho}_{cc}^{(2)} &= \frac{1}{2(r + (1 - \alpha_c)\gamma_a)\Omega_\mu^2} \times (r(4\alpha_c\gamma_a\gamma_{ca} + 2\Omega_\mu^2)\tilde{\rho}_{bb}^{\text{st}} \\ &\quad + i\Omega_c(2(r + \gamma_a)\gamma_{ca} + \Omega_\mu^2)(\tilde{\rho}_{c'c}^{(1)} - \tilde{\rho}_{cc'}^{(1)}) \\ &\quad + \Omega_c\Omega_\mu(r + (1 - \alpha_c)\gamma_a)(\tilde{\rho}_{ac'} + \tilde{\rho}_{c'a})) \end{aligned} \quad (19b)$$

$$\begin{aligned} \tilde{\rho}_{ca}^{(2)} &= \frac{-2ir\alpha_c\gamma_a\tilde{\rho}_{bb}^{\text{st}} + (r + \gamma_a)(\tilde{\rho}_{c'c}^{(1)} - \tilde{\rho}_{cc'}^{(1)})\Omega_c}{2(r + (1 - \alpha_c)\gamma_a)\Omega_\mu} \\ &\quad - \frac{i(\tilde{\rho}_{ac'}^{(1)} - \tilde{\rho}_{c'a}^{(1)})\Omega_c}{4\gamma_{ca}}. \end{aligned} \quad (19c)$$

The next step is to solve for $\tilde{\rho}_{bb}$ and $\tilde{\rho}_{c'c}$ self-consistently, in terms of these steady state solutions. But first we can simplify the expressions already stated using our initial approximations that $r \ll \Omega_c$, $\Omega_b \ll \Omega_\mu$. Moreover, since the ground states are assumed not to decay, $\gamma_{c'c} = \gamma_{c'c}^{\text{ph}}$. We assume that dephasing effects are small, and take $\gamma_{c'c} \ll r$. Note that although we could in principle proceed through the next step of the calculation without making these assumptions, the expressions thus derived are unwieldy. Moreover, these assumptions will be necessary presently when we move to solve to first order in Ω_p/Ω_μ , and so it is expedient (and consistent, given our initial assumptions) to make them now. We

can write,

$$\tilde{\rho}_{c'a}^{(2)} = -\left(\frac{\Omega_c}{\Omega_\mu}\right)\tilde{\rho}_{c'c'} \quad (20a)$$

$$\tilde{\rho}_{c'c}^{(1)} = -\left(\frac{2i\gamma_{c'a}\Omega_c}{\Omega_\mu^2}\right)\tilde{\rho}_{c'c'} \quad (20b)$$

$$\tilde{\rho}_{aa}^{(2)} = \frac{r\Omega_\mu^2\tilde{\rho}_{bb} + 2\gamma_{c'a}\Omega_c^2\tilde{\rho}_{c'c'}}{(1 - \alpha_c)\gamma_a\Omega_\mu^2} \quad (20c)$$

$$\begin{aligned} \tilde{\rho}_{cc}^{(2)} &= \frac{1}{(1 - \alpha_c)\gamma_a\Omega_\mu^2} \times (r\tilde{\rho}_{bb}(\alpha_c\gamma_a\gamma_{ca} + \Omega_\mu^2) \\ &\quad + 2\frac{\Omega_c^2}{\Omega_\mu^2}(2\gamma_{c'a}\Omega_\mu^2 + \gamma_a(4\gamma_{c'a}\gamma_{ca} - (1 - \alpha_c)\Omega_\mu^2))) \end{aligned} \quad (20d)$$

$$\tilde{\rho}_{ca}^{(2)} = \frac{-i(2\gamma_{c'a}\tilde{\rho}_{c'c'}\Omega_c^2 + r\alpha_c\tilde{\rho}_{bb}\Omega_\mu^2)}{(1 - \alpha_c)\Omega_\mu^3} \quad (20e)$$

The equations of motion for $\tilde{\rho}_{bb}$ and $\tilde{\rho}_{c'c}$ can now be written as

$$i\frac{\partial\tilde{\rho}_{bb}}{\partial t} = i(\alpha_b\gamma_a + r)\tilde{\rho}_{aa}^{(2)} - ir\tilde{\rho}_{bb} \quad (21a)$$

$$i\frac{\partial\tilde{\rho}_{c'c}}{\partial t} = i\alpha_{c'}\gamma_a\tilde{\rho}_{aa}^{(2)} + \frac{\Omega_c}{2}(\tilde{\rho}_{c'c}^{(2)} - \tilde{\rho}_{cc'}^{(2)}) \quad (21b)$$

Inserting the expressions for the second order rapidly varying terms and combining the two resulting equations, we find the condition that the steady state populations $\tilde{\rho}_{bb}$ and $\tilde{\rho}_{c'c}$ must satisfy.

$$\tilde{\rho}_{bb} = \frac{2\gamma_{c'a}\alpha_b}{r\alpha_{c'}}\left(\frac{\Omega_c^2}{\Omega_\mu^2}\right)\tilde{\rho}_{c'c'} \quad (22)$$

This condition specifies a unique pair of populations when we impose the additional constraint that the sum of the populations must be 1. Then,

$$\tilde{\rho}_{c'c'} = \frac{r\alpha_c\Omega_\mu^2}{4\alpha_b\gamma_{c'a}\Omega_c^2 + r\alpha_c\Omega_\mu^2}. \quad (23)$$

The other populations, meanwhile, can now be written as

$$\tilde{\rho}_{aa} \approx 0 \quad (24a)$$

$$\tilde{\rho}_{bb} = \tilde{\rho}_{b'b'} \approx \frac{2\alpha_b\gamma_{c'a}\Omega_c^2}{4\alpha_b\gamma_{c'a}\Omega_c^2 + r\alpha_c\Omega_\mu^2} \quad (24b)$$

$$\tilde{\rho}_{cc} \approx 0 \quad (24c)$$

$\tilde{\rho}_{aa}$ and $\tilde{\rho}_{cc}$ vanish because they are of order $\Omega_c^2 r / (\Omega_\mu^2 \gamma_a) \lesssim (\Omega_c / \Omega_\mu)^3 \ll 1$.

From here, the strategy is the same as in the open pumping case, and in fact, the solution in that case carries over wholesale. Eqs. 9, 10, and 11 are general statements in terms of the steady state solutions for $\tilde{\rho}_{aC}$, $\tilde{\rho}_{aC'}$, and the $\tilde{\rho}_{aB}$, $\tilde{\rho}_{aB'}$ terms. In the semi-dressed basis introduced in section II, we now have $\tilde{\rho}_{aC} = \tilde{\rho}_{aC'} = -\frac{\sqrt{2}}{2}\frac{\Omega_c}{\Omega_\mu}\tilde{\rho}_{c'c'}$, just as in the open pumping case; meanwhile $\tilde{\rho}_{BB} = \tilde{\rho}_{B'B'} = \tilde{\rho}_{bb}$, since $\tilde{\rho}_{bb} = \tilde{\rho}_{b'b'}$

and $\tilde{\rho}_{bb'} = 0$. So if we take $\mathfrak{P}_B = \tilde{\rho}_{BB} = \frac{2\alpha_b\gamma_{c'a}\Omega_c^2}{4\alpha_b\gamma_{c'a}\Omega_c^2 + r\alpha_c\Omega_\mu^2}$ and consider the closed pumping solution for $\tilde{\rho}_{c'c'}$, then Eqs. 9-11 hold, now as a function of the pumping from $|b\rangle$ to $|a\rangle$, r .

IV. LINEAR RESPONSE OF THE PUMPED DIGS SYSTEMS

The complex linear susceptibility, expanded about the $|a\rangle \leftrightarrow |b\rangle$ transition, is given by

$$\chi^{(1)} = \frac{2\sigma(\mathbf{r})ND_{ab}\tilde{\rho}_{ab}}{\epsilon_0\mathcal{E}_p} \quad (25)$$

$\chi^{(1)}$ determines both the absorption coefficient, $\alpha(\Delta_p) = k_p\text{Im}[\chi^{(1)}(\Delta_p)]$, and the index of refraction, $n(\Delta_p) \approx$

$(1 + \text{Re}[\chi^{(1)}(\Delta_p)])^{1/2}$. Considerations arising from the particular experimental set-up would determine density profile, $\sigma(\mathbf{r})$, and number density of atoms, N , which are included to formally account for the particular optical thickness of the sample. $D_{ab} = e\langle a|\vec{\epsilon} \cdot x|b\rangle$ is the dipole moment between $|a\rangle$ and $|b\rangle$, as a function of laser polarization, $\vec{\epsilon}$. In our analysis we will focus on the dimensionless reduced susceptibility

$$\tilde{\chi}^{(1)} = \frac{\epsilon_0\hbar\gamma_{ab}}{D_{ab}^2N\sigma(\mathbf{r})}\chi^{(1)} = \frac{2\gamma_{ab}}{\Omega_p}\tilde{\rho}_{ab}. \quad (26)$$

where we have used the definition of the probe Rabi frequency, $\Omega_p = D_{ab}\mathcal{E}_p/\hbar$. This allows us to write the following expression for the linear susceptibility as a function of $\tilde{\rho}_{c'c'}$ and \mathfrak{P}_B , which will vary depending on the pumping configuration.

$$\begin{aligned} \tilde{\chi}^{(1)} = \gamma_{ab} & \left(\frac{(\mathfrak{P}_B(2i\gamma_C - 2\Delta_p - \Omega_b)(2i\gamma_{C'} - 2\Delta_p - \Omega_b) + \Omega_c^2(\tilde{\rho}_{c'c'}^{\text{st}} - \mathfrak{P}_B))}{\Omega_\mu^2(2i\gamma_{C'} - 2\Delta_p - \Omega_b) - (2i\gamma_{ab} - 2\Delta_p - \Omega_b)((i\gamma_C + i\gamma_{C'} - 2\Delta_p - \Omega_b)^2 - \Omega_c^2)} \right. \\ & \left. + \frac{(\mathfrak{P}_B(2i\gamma_C - 2\Delta_p + \Omega_b)(2i\gamma_{C'} - 2\Delta_p + \Omega_b) + \Omega_c^2(\tilde{\rho}_{c'c'}^{\text{st}} - \mathfrak{P}_B))}{\Omega_\mu^2(2i\gamma_{C'} - 2\Delta_p + \Omega_b) - (2i\gamma_{ab} - 2\Delta_p + \Omega_b)((i\gamma_C + i\gamma_{C'} - 2\Delta_p + \Omega_b)^2 - \Omega_c^2)} \right) \quad (27) \end{aligned}$$

As a check on this solution, note that in the limit that $\tilde{\rho}_{c'c'} \rightarrow 0$ (corresponding to $r_{c'} \rightarrow 0$) and $\mathfrak{P}_B \rightarrow 1/2$ (corresponding to normalized population beginning in $|b\rangle$ and $|b'\rangle$), we recover the solution presented in [34], provided that $\gamma_C, \gamma_{C'}$ are small; this latter solution, meanwhile, reduces to the standard EIT solution in the limit that $\Omega_b/\Delta_b, \Omega_c/\Delta_c \rightarrow 0$. Note that it also amounts to an analytic solution to the double dark resonance system, [36], in the limit that $\Omega_b/\Delta_b \rightarrow 0$. (See Appendix D for $\tilde{\chi}^{(1)}$ for arbitrary Δ_μ, Δ_b , and Δ_c)

In section IV A, we will examine the imaginary part of Eq. 27, showing how the system(s) solved above lead to gain lines in the appropriate limits; section IV B will treat the real part of Eq. 27, including the anomalous dispersion present between the gain lines. This discussion requires us to estimate the values for the important variables in the problem. The Rabi frequencies of the coupling laser and RF fields are experimentally tunable over a large range. For the spontaneous emission rate, we take $\gamma_a = 10^7 s^{-1}$ and will measure the Rabi frequencies and detunings in units of γ_{ab} . For the ground state dephasing rates the range of values are limited primarily by collision rates and therefore are temperature and density dependent. However for concreteness, we assume that $\tilde{\gamma}_{ab}, \gamma_C$, and $\gamma_{C'}$ are in the range $10^3 - 10^4 s^{-1}$.

A. $\text{Im}(\chi)$: Gain lines

In Figs. 2 and 3, we plot the imaginary part of the linear susceptibility, Eq. 27, for various choices of pumping rates, in both open and closed cases. In both cases, we compare our analytic results with a direct numerical solution of full density matrix equations of motion. We see that the additional levels manifest themselves as two tunable resonances located inside of the EIT transparency window. In general for arbitrary Δ_b , the new resonances are symmetrically located about $\Delta_p = 0$ at the locations $\Delta_p = \pm\Omega_b^{\text{eff}}/2 = \pm\sqrt{\Delta_b^2 + \Omega_b^2}/2$. For $\Omega_\mu, \gamma_{ab} \gg \Omega_b, \Omega_c, \gamma_C, \gamma_{C'}$, their shape is approximately Lorentzian, given by (for $\Delta_\mu = \Delta_b = 0$):

$$\begin{aligned} \text{Im}[\tilde{\chi}^{(1)}] \approx & \frac{\gamma_{ab}\Omega_c^2}{2\Omega_\mu^2}(\text{Re}(\mathfrak{P}_B) - \tilde{\rho}_{c'c'}^{\text{st}}) \\ & \times \left(\frac{\Omega_c^2/\Omega_\mu^2 + \gamma_{C'}/\gamma_{ab}}{(\Delta_p \mp \Omega_b/2)^2 + (\gamma_{ab}(\Omega_c^2/\Omega_\mu^2 + \gamma_{C'}/\gamma_{ab}))^2} \right) \quad (28) \end{aligned}$$

in the vicinity $\Delta_p \approx \pm\Omega_b/2$. Eq. 28 shows that we can expect absorption for $\text{Re}(\mathfrak{P}_B) > \tilde{\rho}_{c'c'}^{\text{st}}$ and gain for $\tilde{\rho}_{c'c'}^{\text{st}} > \text{Re}(\mathfrak{P}_B)$. Note that these conditions are both necessary and sufficient for absorption and gain, respectively, which implies first that no population need occupy

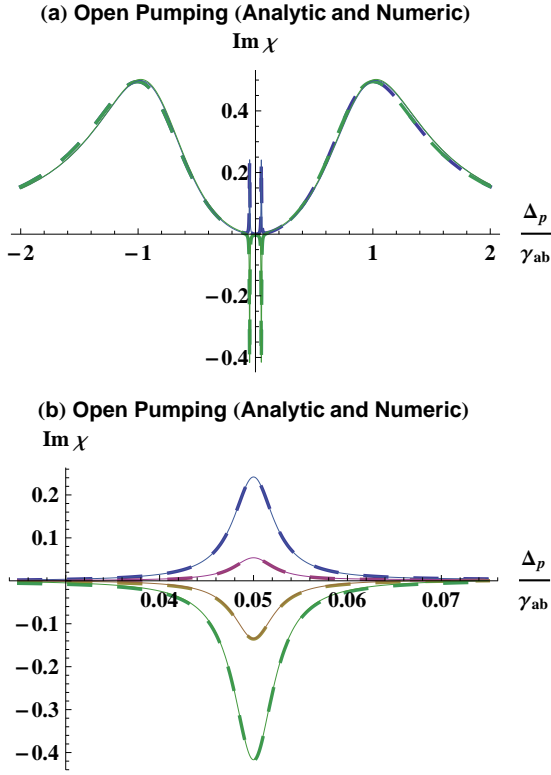


FIG. 2: (Color online) Here we compare analytic and numeric solutions for the imaginary part of the reduced susceptibility (corresponding to the absorption coefficient) in the open pumping case. The numeric solutions are represented by wide dashed lines, and the analytics by narrower solid lines. Agreement between them is quite good. In the top plot, we show the full spectrum in the cases where $r_{c'} = 0$ (absorption lines; blue) and $r_{c'} = .007\gamma_{ab}$ (gain lines; green). In the bottom plot, we show a close up of one of the narrow features. The pumping parameters here, going from top to bottom, are $r_{c'} = 0$ (blue lines), $r_{c'} = .002\gamma_{ab}$ (red lines), $r_{c'} = .004\gamma_{ab}$ (brown lines), and $r_{c'} = .007\gamma_{ab}$ (green lines). In all cases, $r_b = .0001\gamma_{ab}$, $\Omega_b = \Omega_c = .1\gamma_{ab}$, $\Omega_\mu = 2\gamma_{ab}$, and $\gamma_b = \gamma_{b'} = \gamma_c = \gamma_{c'} = 10^{-4}\gamma_{ab}$. We have assumed the dephasings vanish, $\gamma_{jk}^{ph} = 0$.

the excited state in order for amplification to occur (thus, we find amplification without inversion) and second that coherent pumping is not necessary for this amplification to occur. Populations in the appropriate ground states alone are necessary.

In the case of nonzero $\gamma_{c'}$, the widths of the features,

$$\Gamma_n = \gamma_{ab}(\Omega_c^2/\Omega_\mu^2 + \gamma_{c'}/\gamma_{ab}), \quad (29)$$

is the sum of the ‘power broadening’ term $\gamma_{ab}\Omega_c^2/\Omega_\mu^2$ and the dephasing rate for $|c'\rangle$ while the height is given by

$$\text{Im}[\tilde{\chi}^{(1)}(\pm\Omega_b/2)] = \frac{\Omega_c^2\gamma_{ab}(\text{Re}(\mathfrak{P}_B) - \tilde{\rho}_{c'c'}^{\text{st}})}{2(\gamma_{ab}\Omega_c^2 + \Omega_\mu^2\gamma_{c'})}. \quad (30)$$

The dependence on the population $\tilde{\rho}_{c'c'}^{\text{st}}$ is manifest in this expression: the height of the ultranarrow features varies

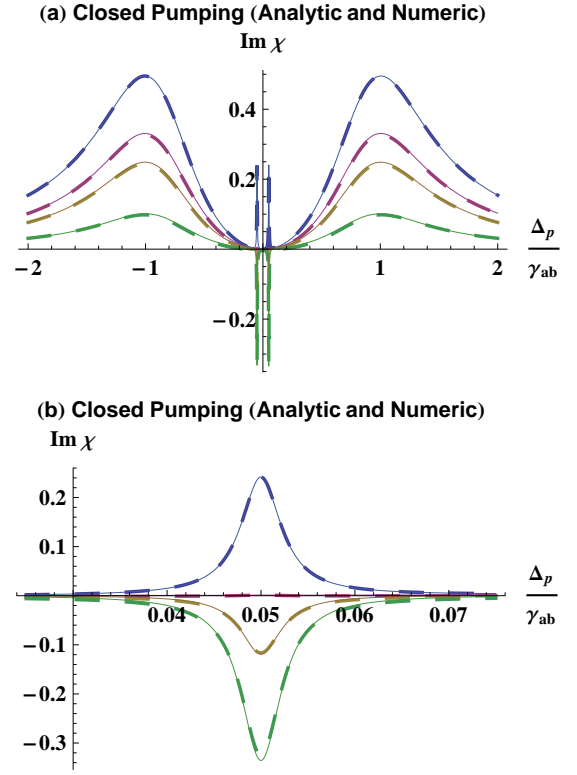


FIG. 3: (Color online) These are analytic and numeric solutions for the imaginary part of the susceptibility in the closed pumping case. Again, the numeric solutions are represented by wide dashed lines, and the analytics by narrower solid lines. The top plot shows the full spectrum as we vary r ; the bottom plot show a close up of one of the narrow features. In both plots, moving from the top curve to the bottom, the parameters are $r = 0$ (blue lines), $r = .005\gamma_{ab}$ (red lines), $r = .01\gamma_{ab}$ (brown lines), and $r = .04\gamma_{ab}$ (green lines). In all cases, $\Omega_b = \Omega_c = .1\gamma_{ab}$, $\Omega_\mu = 2\gamma_{ab}$, and $\gamma_C = \gamma_{C'} = \gamma_{c'c'} = \gamma_{b'b} = 10^{-4}\gamma_{ab}$.

linearly with the difference in populations between $|b\rangle$ (or in general a function of the population of $|b\rangle$) and $|c'\rangle$. When the population in $|c'\rangle$ becomes large, the sign of the Lorentzian reverses, and the absorption line becomes a gain line.

The populations $\tilde{\rho}_{c'c'}$ and $\text{Re}(\mathfrak{P}_B)$ vary with the pumping rates for each of the two pumping configurations. In the open pumping case, the relationships are linear in the pumping rates r_b and $r_{c'}$; the other states do not attain appreciable population. We find gain when

$$\frac{r_{c'}}{r_b} > \frac{(2\gamma_{c'a}\Omega_c^2 + \gamma_{c'}\Omega_\mu^2)}{(\gamma_b + \gamma_{b'})\Omega_\mu^2}. \quad (31)$$

The linear dependence on the pumping rate in the open pumping configuration permits additional control over the shapes of the lines. As can be seen in Eq. 30, the heights of the features are proportional to Ω_c^2 . In the case where Ω_c becomes small (as is necessary to narrow the widths of the features), it is theoretically possible to counteract the corresponding suppression of the feature’s

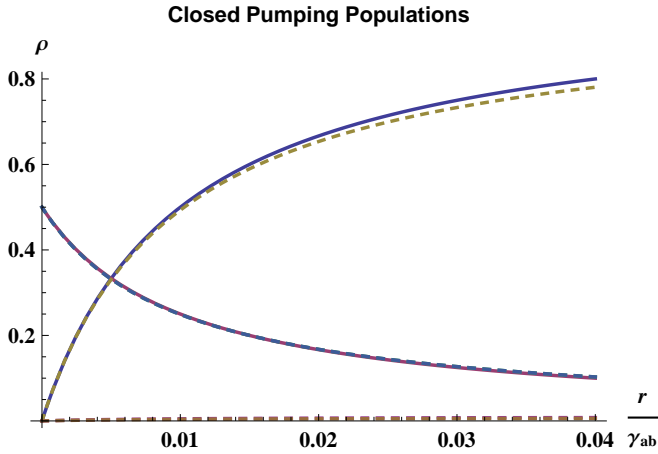


FIG. 4: (Color online) The analytic solutions (solid lines) for the populations in the closed pumping case, plotted with numerical solutions (dashed lines) to the full system of equations. The lines with positive slope are the population of $|c'\rangle$ in each case; the other non-zero lines are the populations of $|b\rangle, |b'\rangle$. The dashed lines with vanishing population correspond to $|a\rangle$ and $|c\rangle$. In all cases, $\Omega_b = \Omega_c = .1\gamma_{ab}$, $\Omega_\mu = 2\gamma_{ab}$, and $\gamma_C = \gamma_{C'} = \gamma_{c'} = \gamma_{b'b} = 10^{-4}\gamma_{ab}$.

height by increasing the pumping rates r_b (for absorption) or $r_{c'}$ (for gain).

In the closed pumping configuration, meanwhile, the populations depend on a single parameter, r . Now we find gain for

$$r > \frac{2\alpha_b\gamma_{c'a}\Omega_c^2}{\alpha_c\Omega_\mu^2}. \quad (32)$$

Here, it is useful to compare the analytic expressions for the populations to the populations found by direct numerical calculation (see Fig. 4). As we see, there is excellent agreement in the case of small r , as assumed. As r grows, both plots plateau, but there is a small deviation between the numerics and analytics. This arises because we assumed $r \ll \Omega_b, \Omega_c$. Indeed, it is surprising that agreement is acceptable for $r \gtrsim \Omega_b, \Omega_c$ in these plots.

In the case where $\tilde{\rho}_{c'c}$ becomes large, the presence of gain lines without population inversion can be understood in terms of dressed states. Again assuming $\Delta_c = 0$ and $\Delta_\mu = 0$, the eigenstates of the Hamiltonian for the $\{|a\rangle, |c\rangle, |c'\rangle\}$ subsystem, $H' = \hbar\omega_a(|a\rangle\langle a| + |c\rangle\langle c| + |c'\rangle\langle c'|) - (\hbar/2)(\Omega_\mu|a\rangle\langle c| + \Omega_c|c'\rangle\langle c| + h.c.)$, are

$$|a_+\rangle = \frac{1}{\sqrt{2}}(\sin\theta|a\rangle + |c\rangle + \cos\theta|c'\rangle) \quad (33)$$

$$|a_-\rangle = \frac{1}{\sqrt{2}}(\sin\theta|a\rangle - |c\rangle + \cos\theta|c'\rangle) \quad (34)$$

$$|a_0\rangle = \cos\theta|a\rangle - \sin\theta|c'\rangle \quad (35)$$

where $\tan\theta = \Omega_\mu/\Omega_c$. The energies of the states $|a_\pm\rangle$ are $E_\pm = \hbar\omega_a \pm \hbar\sqrt{\Omega_\mu^2 + \Omega_c^2}/2$ while $|a_0\rangle$ has energy $E_0 = \hbar\omega_a$. Note that $\{|a\rangle, |c\rangle, |c'\rangle\}$ is isomorphic to a Λ

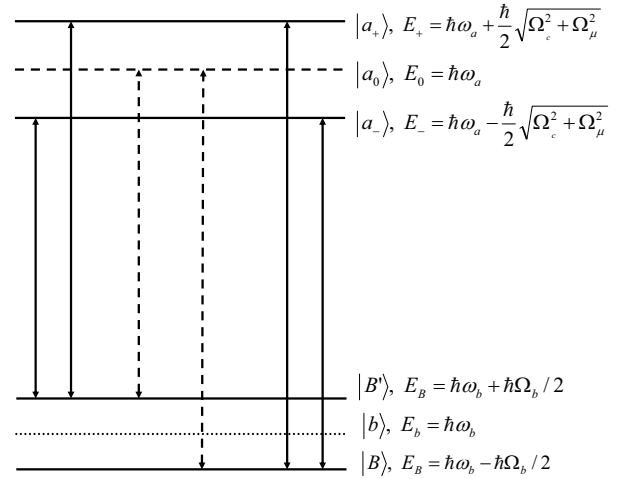


FIG. 5: Energy level diagram that indicates transitions induced by the probe laser between the ground state manifold $\{|B\rangle, |B'\rangle\}$ and the excited state manifold $\{|a_+\rangle, |a_-\rangle, |a_0\rangle\}$. Transitions to the gain state $|a_0\rangle$ are indicated by dashed lines. The energy of the bare state $|b\rangle$ is also shown for reference.

atom and so $|a_0\rangle$ is a dark state of the sort familiar from STIRAP and coherent population trapping. To distinguish it from the more familiar dark state composed of $|b\rangle$ and $|c\rangle$ responsible for EIT, we will call $|a_0\rangle$ the gain state. Fig. 5 shows a schematic diagram of the energy levels of the dressed ground state manifold $\{|B\rangle, |B'\rangle\}$, which are coupled to all three states of the excited state manifold $\{|a_+\rangle, |a_-\rangle, |a_0\rangle\}$ via the probe.

The eigenstate $|a_0\rangle$ is decoupled from the control laser, so there will not be any destructive quantum interference in the probe absorption or emission for transitions to $|a_0\rangle$. This explains why we find spectral lines at the locations corresponding to transitions from $|B\rangle$ and $|B'\rangle$ to $|a_0\rangle$. Moreover, in the limit as $\Omega_c \ll \Omega_\mu$, we find $\sin\theta \gg \cos\theta$, and so $|a_0\rangle \approx |c'\rangle$. Thus in the dressed state basis, the population in $|c'\rangle$ corresponds to large population in the gain state. The gain state energy remains $\hbar\omega_a$, however, even in this limit, which means that although there is no population inversion in the bare state basis, there is large inversion in this dressed state basis. Whereas when the population in $|c'\rangle$ is small, transitions from the $\{|B\rangle, |B'\rangle\}$ manifold to $|a_0\rangle$ lead to absorption resonances at $\omega_a - \omega_{B,B'}$. These change to gain lines as the population in $|c'\rangle \approx |a_0\rangle$ increases.

It is worth emphasizing that the gain lines described here arise from different physical process than, say, standard driven two level pump-probe spectroscopy. There, gain arises from the exchange of light quanta between the strong pump field and the weak probe. The dressed states used to describe and explain pump-probe spectroscopy necessarily involve the probed transition. Here, the basis in which the gain state emerges does not include the probed transition. In the present system, the gain is due to stimulated emission from a metastable quantum state,

$|a_0\rangle$, to a decoupled (to zeroth order in Ω_p/Ω_μ) ground state. It is the coherent preparation of the $\{|a\rangle, |c\rangle, |c'\rangle\}$ manifold that permits emission from this state (essentially $|c'\rangle$, in the limits we have considered) even though the population of the bare excited state is negligible.

The mechanism here also differs from textbook amplification without inversion, as presented for instance by Scully and Zubairy [47]. There gain occurs because the coherence between the ground states of the Λ atom ($|b\rangle$ and $|c\rangle$, here) cancels absorption, leaving only stimulated emission. Thus standard inversionless amplification system requires coherent pumping. This permits gain even in the presence of small population of the excited state, $|a\rangle$. But crucially, *some* population in the excited state is necessary. In the present system, $|a\rangle$ may have zero population, so long as $|c'\rangle$ is populated. We note that there are other approaches to amplification without inversion (which is ultimately a term that describes systems exhibiting a certain property, rather than the name of a particular class of systems) that are closer in spirit to the current system [46]. But it is nonetheless worthwhile to distinguish the DIGS approach from the “standard” amplification without inversion, since their mutual connection to Λ type atoms may produce confusion.

B. $\text{Re}(\chi)$: Anomalous dispersion

When the pumping rate is such that the gain peaks are large we find a region of anomalous dispersion but low absorption. This result should be unsurprising, as the Kramers-Kronig relations guarantee that any pair of sufficiently narrow and tall gain lines will give rise to anomalous dispersion, given the analyticity of the susceptibility [10]. The dispersion is proportional to the first derivative of the linear susceptibility. In the present case, the heights, widths, and separation of the peaks, and thus the magnitude and range of the anomalous dispersion, are all tunable by varying r (or r_b and $r_{c'}$), Ω_b , and Ω_c . The real part of the susceptibility is shown for several values of the pumping rate in Fig. 6. Our definition of the probe detuning,

$$\Delta_p = \omega_a - \omega_b - \nu_p,$$

implies that the dispersion is anomalous when the slope of the real part of χ is *positive*.

Near the bare transition frequency, $\Delta_p = 0$, the real part of the susceptibility is approximately linear. To second order in Ω_b/Ω_μ and Ω_c/Ω_μ (the order to which the solution for the susceptibility is valid), we find,

$$\text{Re}(\tilde{\chi}^{(1)}) = \frac{4\gamma_{ab}(\Omega_c^2 \tilde{\rho}_{c'c'} - \text{Re}(\mathfrak{P}_B)(\Omega_b^2 + \Omega_c^2))}{\Omega_b^2 \Omega_\mu^2} \Delta_p. \quad (36)$$

See Fig. 7 for a comparison of this linear solution and the full real part of the susceptibility for several populations. This relation can be rewritten to reflect the relative populations necessary for dispersion to become anomalous.

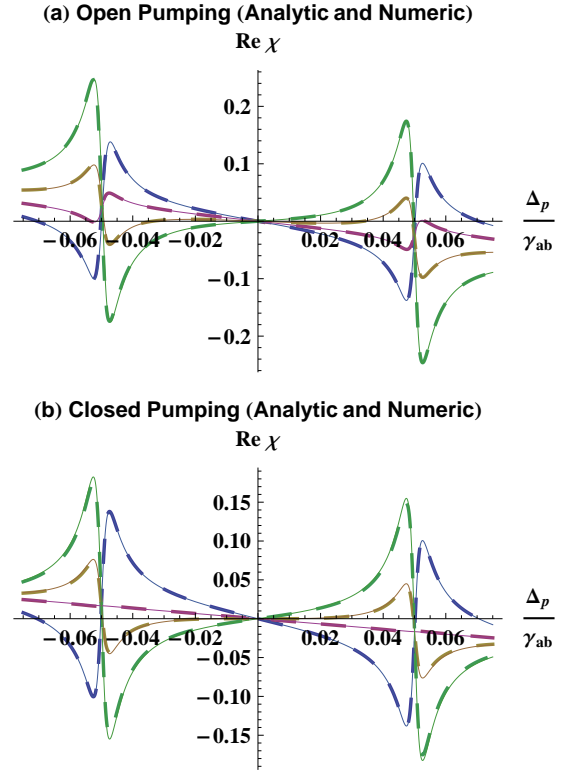


FIG. 6: (Color online) Here we compare our analytic and numeric solutions for various pumping rates in the open configuration (a) and closed configuration (b) in the vicinity of the new features. In both cases, we see that increasing the pumping (or, increasing pumping to $|c'\rangle$) results in a change from normal dispersion (negative slope, on our sign conventions) to anomalous dispersion (positive slope) in the region around zero detuning. Once again, the analytic solutions are represented by narrow solid lines, and the numerics by wide dashed lines. The parameters in both cases are the same as in the close-ups in Figs. 2 (b) and 3 (b). In particular, for (a) we have (from most negative slope to most positive), $r_{c'} = 0$ (blue lines), $r_{c'} = .002\gamma_{ab}$ (red lines), $r_{c'} = .004\gamma_{ab}$ (brown lines), and $r_{c'} = .007\gamma_{ab}$ (green lines). For (b), we have $r = 0$ (blue lines), $r = .002\gamma_{ab}$ (red lines), $r = .004\gamma_{ab}$ (brown lines), and $r = .007\gamma_{ab}$ (green lines).

The dispersion is anomalous just in case

$$\frac{\tilde{\rho}_{c'c'}}{\text{Re}(\mathfrak{P}_B)} > 1 + \frac{\Omega_b^2}{\Omega_c^2}. \quad (37)$$

Eq. 37 can be rewritten as a constraint on r_b and $r_{c'}$ in the opening pumping case and r in the closed pumping case by substituting the expressions for the populations derived in sections III A and III B. In the open pumping case, the constraint on $r_{c'}/r_b$ is given by

$$\frac{r_{c'}}{r_b} > \frac{(2\gamma_{c'a}\Omega_c^2 + \gamma_{c'}\Omega_\mu^2)(\Omega_b^2 + \Omega_c^2)}{(\gamma_b + \gamma_{b'})\Omega_\mu^2\Omega_c^2}, \quad (38)$$

whereas the corresponding constraint on r in the closed

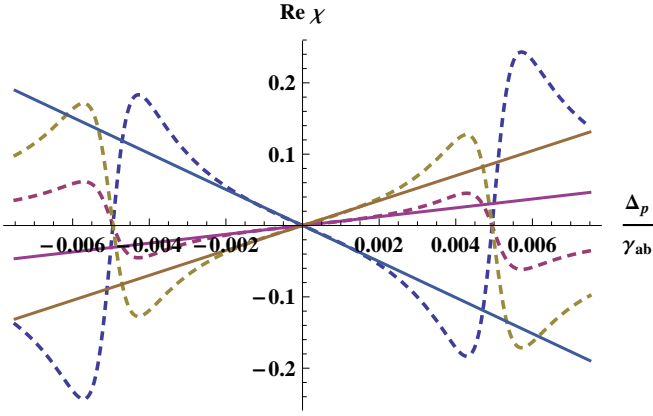


FIG. 7: (Color online) Here we compare our linear approximation of the real part of the susceptibility, Eq. 36, (solid lines) with the general analytic solution, Eq. 27 (dashed lines) for various populations. For complete generality, and because the purpose is to show agreement between the linear approximation and the full susceptibility, we consider the populations directly, here, rather than limiting ourselves to one pumping scheme or another. In order from most negative to most positive slopes, we have $\mathfrak{P}_B = 1$ and $\tilde{\rho}_{c'c'} = 0$ (blue lines); $\mathfrak{P}_B = .25$ and $\tilde{\rho}_{c'c'} = .5$ (red lines); and $\mathfrak{P}_B = .1$ and $\tilde{\rho}_{c'c'} = .8$ (brown lines). In all plots, $\gamma_C = \gamma_{C'} = \gamma_{ab} \times 10^{-4}$, $\Omega_\mu = 2\gamma_{ab}$, $\Omega_b = \Omega_c = \gamma_{ab}/10$.

pumping case is given by,

$$r > \frac{2\alpha_b\gamma_{c'a}(\Omega_b^2 + \Omega_c^2)}{\alpha_c\Omega_\mu^2}. \quad (39)$$

It is tempting to consider the limit that $\Omega_b^2/\Omega_c^2 \rightarrow 0$. However, Eqs. 36 and 37 are not valid in this limit. For one, taking $\Omega_b \rightarrow 0$ makes sense in the context of Eq. 37, but not Eq. 36. More importantly, the assumption of linearity only holds when there is a transparency window between the two peaks, or roughly when $\Omega_c^2/\Omega_\mu^2 \ll \Omega_b/\gamma_{ab}$, which corresponds to the case where the separation of the peaks is larger than their widths. It follows that, while inversion of the populations of $|a_0\rangle \approx |c'\rangle$ and $|b\rangle$ is sufficient to produce gain lines, the constraint on the population of $|a_0\rangle$ necessary for anomalous dispersion is more stringent. This result can be seen clearly in comparing Eqs. 38 and 39 to the corresponding expressions in section IV A, Eqs. 31 and 32. The pumping rate necessary for producing anomalous dispersion increases as the square of the width of the window between the peaks, supposing that the widths of the peaks are held constant. Thus, though it is in principle possible to produce wide spectral regions of anomalous dispersion, there is a practical barrier imposed by how rapidly one can pump atoms into $|c'\rangle$.

A distinctive and important feature of Eq. 36 is that the dispersion does not depend on the dephasings γ_C and $\gamma_{C'}$. This result is not a relic of the approximations that went into deriving the linearized equation, as can be seen in Fig. 8. The effect of dephasing between $|c'\rangle$

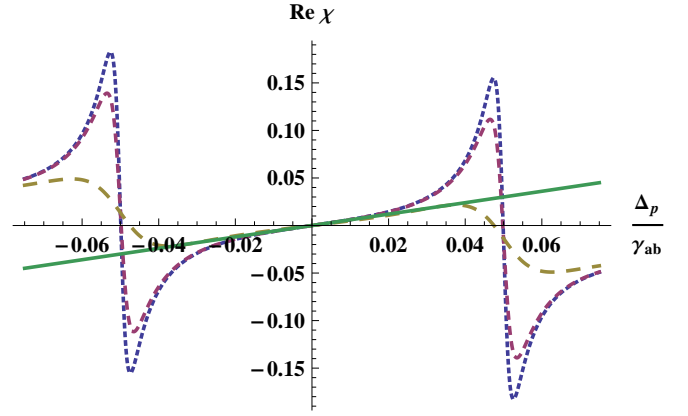


FIG. 8: (Color online) Here we compare our linear approximation of the real part of the susceptibility, Eq. 36, with the general analytic solution, Eq. 27, as dephasing increases. The (blue) dotted line has $\gamma_C = \gamma_{C'} = \gamma_{ab} \times 10^{-4}$; the (red) dashed line has $\gamma_C = \gamma_{C'} = \gamma_{ab} \times 10^{-3}$; the (yellow) broad-dashed line has $\gamma_C = \gamma_{C'} = \gamma_{ab}/100$. The solid (green) line is the linear approximation. Note that although the susceptibility is depressed in the vicinity of the new resonances as the dephasing increases, the dispersion in the linear regime does not change. In all plots, we take the generalized populations $\tilde{\rho}_{c'c'} = .8$ and $\text{Re}(\mathfrak{P}_B) = .1$, while other parameters are $\Omega_\mu = 2\gamma_{ab}$, $\Omega_b = \Omega_c = \gamma_{ab}/10$.

and $\{|b\rangle, |b'\rangle\}$ is to destroy the coherences responsible for producing the new narrow resonances. But even as the resonances shrink, the region between the peaks near zero detuning remains unchanged, until $\gamma_{C'} \gg \Omega_c$ and the resonances vanish altogether.

The values of the anomalous dispersion that we predict have dramatic consequences for group velocity, which in the current context can be written $v_g = c/n_g$, where n_g is the group velocity index,

$$n_g = n - \frac{\nu_p}{2n} \frac{\partial \text{Re}(\chi^{(1)})}{\partial \Delta_p}.$$

$n = (1 + \text{Re}(\chi^{(1)}))^{1/2}$ is the index of refraction, as defined above. The absolute value of the dispersion in the anomalous regime, for large population $|c'\rangle$, is comparable to the magnitude of EIT dispersion, as can be seen by examining Eq. 36. In the case where $\mathfrak{P}_B = 1/2$, the dispersion becomes approximately that of “standard EIT,” which we take to be EIT in an identical system, without the two additional fields/levels we have introduced here.

$$\frac{\partial \text{Re}(\tilde{\chi}^{(1)})}{\partial \Delta_p} = -\frac{4\gamma_{ab}\text{Re}(\mathfrak{P}_B)(\Omega_b^2 + \Omega_c^2)}{\Omega_b^2\Omega_\mu^2}. \quad (40)$$

In the opposite limit, of very large pumping, $\tilde{\rho}_{c'c'} \rightarrow 1$ and we find

$$\frac{\partial \text{Re}(\tilde{\chi}^{(1)})}{\partial \Delta_p} = \frac{4\gamma_{ab}\Omega_c^2\tilde{\rho}_{c'c'}}{\Omega_b^2\Omega_\mu^2} \quad (41)$$

For $\Omega_c = \Omega_b$, Eq. 41 reduces to the expression for EIT dispersion, with opposite sign. This means that if one

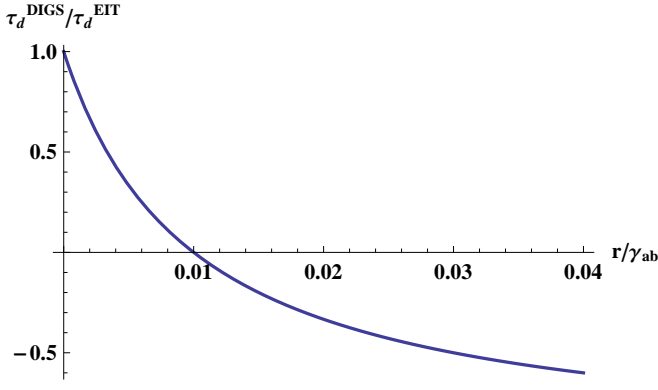


FIG. 9: The ratio $\tau_d^{\text{DIGS}}/\tau_d^{\text{EIT}}$ as a function of the closed pumping rate, r/γ_{ab} . We see that for $r > \gamma_{ab}/10$, the time delay becomes negative; for $r > 3\gamma_{ab}/10$, the magnitude of the negative time delay comes within a factor of 2 of the EIT time delay, permitting much faster light than previously observed. Here $\Omega_b = \Omega_c = 0.1\gamma_{ab}$

begins with a suitable EIT system and then introduces the additional couplings and pump processes, one can generate negative group velocities of the same magnitude as the ultraslow light observed by [50], [43], and [51].

Negative group velocities can best be understood in terms of the group delay,

$$\tau_d = \ell(1/v_g - 1/c)$$

where ℓ is the sample thickness. To see the point made at the end of the last paragraph most clearly, suppose that a given EIT system exhibits a group delay of τ_d^{EIT} . Then, for index of refraction $n \approx 1$ (as we have here) we can expect a group delay in the same system prepared with the additional DIGS couplings of,

$$\tau_d^{\text{DIGS}} = \tau_d^{\text{EIT}} \frac{\text{Re}(\mathfrak{P}_B)(\Omega_b^2 + \Omega_c^2) - \Omega_c^2 \tilde{\rho}_{c'c'}}{\Omega_b^2}. \quad (42)$$

We plot $\tau_d^{\text{DIGS}}/\tau_d^{\text{EIT}}$ as a function of the closed pumping rate in Fig. 9.

To be perfectly concrete, take as a sample system the ^{87}Rb vapor cell prepared in [43], modified to include the additional couplings (see section VI). We can assume that $\Omega_b \approx \Omega_c$, so that the details of the strengths of the couplings are irrelevant. They observe group velocities of 90m/s through their 2.5cm long sample, corresponding to a group delay of .26ms. In the corresponding DIGS system, with pumping such that $\tilde{\rho}_{c'c'} \approx .8$ and $\mathfrak{P}_B \approx .1$ (this corresponds to a closed pumping rate of approximately $r = .04\gamma_{ab}$ for $\Omega_b \approx \Omega_c \approx .1\gamma_{ab}$ and $\Omega_\mu = 2\gamma_{ab}$), we should expect a group velocity of -150m/s, corresponding to a group delay of -.156ms and a group velocity index of $n_g = -2 \times 10^6$. These numbers represent an improvement of four orders of magnitude over Ref. [8], who found a group velocity index of $n_g \approx -310$, and of two orders of magnitude over Ref. [44] who observed a group velocity index of $n_g = -14\,400$ in a Cs atomic va-

por system. This latter result is the largest superluminal group velocity yet observed directly.

V. DOPPLER BROADENING

Doppler broadening is an important experimental constraint on the current system. Thus far, we have disregarded Doppler broadening in our treatments of DIGS systems, and so we will focus on it here. For a single photon with wave vector \vec{k} incident on an atom moving with velocity \vec{v} , the Doppler effect shifts the atomic transition frequency ω_0 by

$$\omega_D = \omega_0 + \vec{k} \cdot \vec{v}.$$

The ‘‘Doppler width,’’ then, is given by the width of the atomic velocity distribution $\sigma_D = \langle (\omega_D - \omega_0)^2 \rangle = \omega_0 \sigma_v / c$. For a Maxwell-Boltzmann distribution σ_v is given by (FWHM)

$$\sigma_v = 2\sqrt{2 \ln 2} \frac{k_B T}{m}$$

where k_B is the Boltzmann constant, T is the temperature, and m is the mass of the atoms.

From these considerations, we conclude that Doppler shifts will be unimportant for the RF fields. Working, for instance, at room temperature ($T = 300\text{K}$), in a gas of Rubidium atoms, we would find that $\sigma_v \approx 400\text{m/s}$. For an RF field, we can take $\omega_0 \sim 100\text{MHz}$, which gives an estimation of the Doppler width at $\sigma_D \sim 100\text{Hz}$. Thus for the RF fields, the effect of Doppler broadening will be much less than the homogeneous broadening from dephasing (which we have thus far estimated in our plots at $\gamma_b, \gamma_{b'}, \gamma_c, \gamma_{c'} \approx 10^{-4}\gamma_{ab} \approx 10^3\text{Hz}$). In the same gas, however, taking $\omega_0 \approx 1\text{PHz}$ —a characteristic frequency of light—we find that the Doppler width will be approximately $\sigma_D \approx 1\text{GHz} \gg \gamma_{ab}$. Thus Doppler broadening will dominate the optical transitions $\{|b\rangle, |b'\rangle\} \leftrightarrow |a\rangle$ and $\{|c\rangle, |c'\rangle\} \leftrightarrow |a\rangle$. In a laser cooled system, where $T \approx 1\mu\text{K} - 100\mu\text{K}$, the Doppler width would be reduced to approximately $\gamma_{ab}/10 - \gamma_{ab}/100$.

We can model the Doppler broadening by averaging over a Gaussian distribution of the one photon probe detuning Δ_p and the two photon detuning, $\delta = \Delta_p - \Delta_\mu$. Written in terms of these two detunings (see appendix D for a full statement of the susceptibility including all nonzero detunings) the Doppler broadened susceptibility as a function of the mean probe detuning, Δ_p , with mean pump detuning fixed at 0 is given by

$$\tilde{\chi}_D^{(1)}(\Delta_p) = \frac{1}{2\pi\sigma_{\Delta_p}\sigma_\delta} \int_{-\infty}^{\infty} \int_{-\infty}^{\infty} d\Delta'_p d\delta \tilde{\chi}^{(1)}(\Delta'_p, \delta) \times e^{-(\Delta'_p - \Delta_p)^2 / (2\sigma_{\Delta_p}^2)} e^{-(\delta - \Delta_p)^2 / (2\sigma_\delta^2)}. \quad (43)$$

Evaluating Eq. 43 numerically for a variety of variances (see Figs. 10 and 11), we can draw several conclusions about the constraints imposed by Doppler broadening. For one, the narrow features are unaffected by the

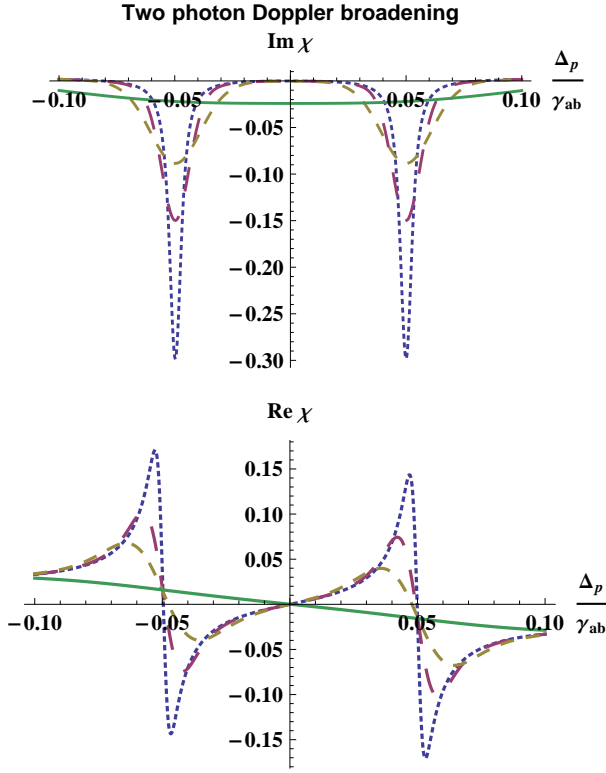


FIG. 10: (Color online) Here we have the two photon Doppler effect on the real and imaginary parts of the susceptibility near the narrow features. In both plots, we keep the one photon variance constant (to clarify the effect of the two photon broadening) at $\sigma_{\Delta_p} = .001\gamma_{ab}$. The formatting of the lines is consistent between the two plots. In both, the blue dotted line corresponds to $\sigma_{\delta} = .001\gamma_{ab}$, the red dashed line has $\sigma_{\delta} = .005\gamma_{ab}$, the brown dashed line has $\sigma_{\delta} = .01\gamma_{ab}$, and the solid green line (for which the features have vanished altogether) has $\sigma_{\delta} = .05\gamma_{ab}$. For simplicity and generality, we have used generalized populations rather than particular models for open or closed pumping, with $\mathfrak{P}_B = .1$ and $\tilde{\rho}_{c'c'} = .8$, and we have allowed the dephasings γ_C and $\gamma_{C'}$ to vanish. The other parameters are $\Omega_{\mu} = 2\gamma_{ab}$, $\Omega_b = \Omega_c = \gamma_{ab}/10$.

single photon broadening, at least while $\sigma_{\Delta_p}/\gamma_{ab} \lesssim 1$. To see why this would be, consider the expansion of $\text{Im}(\tilde{\chi}^{(1)})$ around $\pm\Omega_b/2$ in terms of the one and two photon detunings. We find,

$$\text{Im}(\tilde{\chi}^{(1)}(\Delta_p, \delta)) \approx \frac{\gamma_{ab}\Omega_c^2}{2\Omega_{\mu}^2} (\text{Re}(\mathfrak{P}_B) - \tilde{\rho}_{c'c'}^{\text{st}}) \times \left(\frac{\gamma_{ab}\Omega_c^2/\Omega_{\mu}^2 + \gamma_{C'}}{(\gamma_{ab}\Omega_c^2/\Omega_{\mu}^2 + \gamma_{C'})^2 + (\delta \mp \Omega_b/2 + \Omega_c^2/\Omega_{\mu}^2(\Delta_p \mp \Omega_b/2))^2} \right) \quad (44)$$

Under the assumptions that $\Omega_c^2/\Omega_{\mu}^2 \ll 1$ and $\Delta_{\mu} \rightarrow 0$, this expression reduces to the Lorentzian given in Eq. 28. In this case, Eq. 44 depends on δ alone (because the term $\Omega_c^2/\Omega_{\mu}^2(\Delta_p \mp \Omega_b/2)$ can be neglected in the denominator), which explains why the widths of the features are more

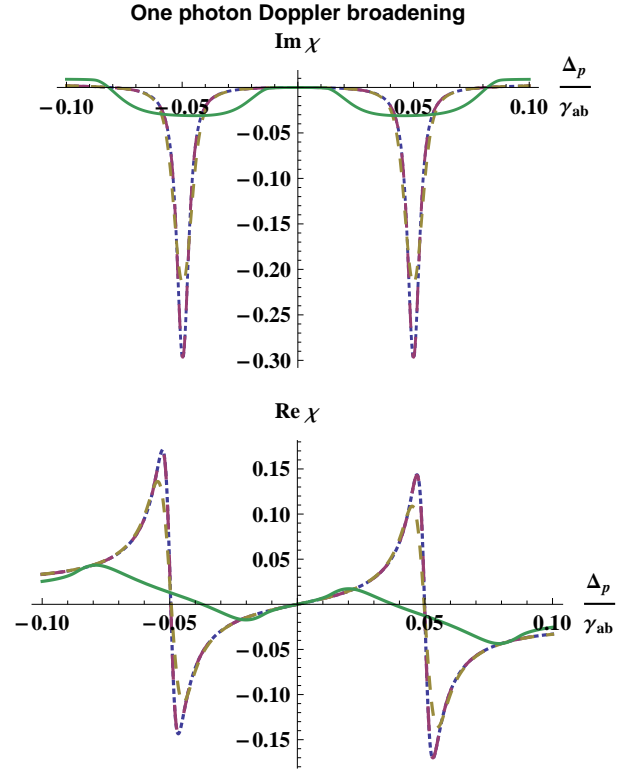


FIG. 11: (Color online) The one photon Doppler effect. Again, we keep the two photon broadening constant at $\sigma_{\delta} = .001\gamma_{ab}$. In this case we show a wide array of values for σ_{Δ_p} , as the features are much less sensitive to the one photon broadening than the two photon broadening—indeed, each line represents variance an order of magnitude larger than the last. In both the top and bottom plots, the blue dotted line corresponds to $\sigma_{\Delta_p} = .01\gamma_{ab}$, the red dashed line has $\sigma_{\Delta_p} = .1\gamma_{ab}$, the brown dashed line has $\sigma_{\Delta_p} = \gamma_{ab}$, and the solid green line has $\sigma_{\Delta_p} = 10\gamma_{ab}$. For simplicity and generality, we have once again used generalized populations rather than particular models for open or closed pumping, with $\mathfrak{P}_B = .1$ and $\tilde{\rho}_{c'c'} = .8$, and we have allowed the dephasings γ_C and $\gamma_{C'}$ to vanish. The other parameters are $\Omega_{\mu} = 2\gamma_{ab}$, $\Omega_b = \Omega_c = \gamma_{ab}/10$.

sensitive to inhomogeneous broadening of the two photon transition. Meanwhile, when $\sigma_{\Delta_p}\Omega_c^2/\Omega_{\mu}^2$ approaches the width of the features, broadening of the single photon process becomes important. Nevertheless, even for $\sigma_{\Delta_p}/\gamma_{ab} \approx 10$, our numerics show that the features will persist, albeit in suppressed form.

The narrow features are far more sensitive to the two photon broadening. When σ_{δ} approaches the widths of the features, $\gamma_{ab}\Omega_c^2/\Omega_{\mu}^2 + \gamma_{C'}$, they are rapidly broadened and ultimately washed out. One possible way of avoiding this difficulty is to work with a Doppler-free geometry, where the probe and the control lasers are copropagating. In this case, the two photon broadening vanishes and it would be possible to observe the (one photon broadened) narrow resonances even in a room temperature system, as per the discussion in the previous paragraph. It would

also be possible to work in a system with two photon Doppler broadening, so long as the temperature is sufficiently low. For $\Omega_c^2/\Omega_\mu^2 \approx .01$, it would be possible to work in a laser cooled system; for smaller Ω_c/Ω_μ , a quantum degenerate system would be necessary to realize the gain.

The anomalous dispersion, meanwhile, is more robust under Doppler broadening. Just as when one increases the homogeneous broadening of the narrow lines, the slope of the real part of the susceptibility in the anomalous regime is unchanged even for large inhomogeneous broadening. It is only when the features are washed out entirely by the inhomogeneous broadening that the anomalous dispersion is lost. In particular, the anomalous dispersion is not reduced when the variance in the one photon detuning, σ_{Δ_p} , is as large as $10\gamma_{ab}$. The dispersion is more sensitive to the two photon detuning, but only because the features themselves vanish entirely for a smaller value of σ_δ . This means that the anomalous dispersive regime should be readily observable and unsuppressed even in a room temperature gas, provided one uses a Doppler-free geometry to eliminate the two photon broadening. Our numerical calculation predicts that even in the absence of co-propagating lasers, the dispersion will be unchanged for $\sigma_\delta \lesssim \gamma_{ab}/100$, even though the resonances will be severely broadened. Thus it should be possible to observe the anomalous dispersion in a laser-cooled gas without a Doppler-free geometry.

VI. SUMMARY AND CONCLUSIONS

As a final note on experimental realizability, we propose several possible level structures. The levels we propose here are for ^{87}Rb , though the equivalent levels in ^{23}Na would work equally well. The first proposal is a modification of the structure used in the EIT experiment in Ref. [43], which we used above to make numerical predictions for the values of the negative group delay in our system. For the closed pumping system, one might use D_1 line with $|a\rangle = |5P_{1/2}, F = 2, m_f = 2\rangle$, $|b\rangle = |5S_{1/2}, F = 1, m_f = 1\rangle$, $|b'\rangle = |5S_{1/2}, F = 1, m_f = 0\rangle$, $|c\rangle = |5S_{1/2}, F = 2, m_f = 1\rangle$, and $|c'\rangle = |5S_{1/2}, F = 2, m_f = 2\rangle$. Alternatively, one might use the D_2 line with $|a\rangle = |5P_{3/2}, F = 2, m_f = 2\rangle$ and the same ground states from the $5S_{1/2}$ manifold as just given for the D_1 line. Then $|a\rangle$ decays only to $|b\rangle$, $|c\rangle$, and $|c'\rangle$, as described by our model. (Note that choosing levels where $|a\rangle$ decays also to $|b'\rangle$ will not change qualitatively any of our results provided $\Omega_b \neq 0$ and $\Delta_b = 0$.) For both of the configurations we propose, both the probe and the control beam would have to be σ_+ polarized.

In conclusion, we have studied the effects of various pumping configurations on the linear response of a driven five-level atom. We have found that when the population of one of the ground states, $|c'\rangle$, becomes large, it produces two amplification resonances without population inversion in the bare state basis. We analyzed the depen-

dence of the population of $|c'\rangle$ on two different pumping configurations. Moreover, we have shown that in the region between the two gain lines, it is possible to tune the system to permit anomalous dispersion. We have studied the effects of Doppler broadening on this system, and concluded that the anomalous dispersion is robust under both homogeneous and inhomogeneous broadening of the gain lines, so long as the gain lines do not vanish.

C.P.S. acknowledges support for this work from the National Science Foundation award no. 0757933.

APPENDIX A

The equations of motion for the system described in section II are given by,

$$i \frac{\partial \tilde{\rho}_{aa}}{\partial t} = -\frac{\Omega_\mu}{2}(\tilde{\rho}_{ca} - \tilde{\rho}_{ac}) + \frac{\Omega_p}{2}(\tilde{\rho}_{ab} - \tilde{\rho}_{ba}) \quad (\text{A1a})$$

$$i \frac{\partial \tilde{\rho}_{bb}}{\partial t} = \frac{\Omega_b}{2}(\tilde{\rho}_{bb'} - \tilde{\rho}_{b'b}) - \frac{\Omega_p}{2}(\tilde{\rho}_{ab} - \tilde{\rho}_{ba}) \quad (\text{A1b})$$

$$i \frac{\partial \tilde{\rho}_{b'b'}}{\partial t} = -\frac{\Omega_b}{2}(\tilde{\rho}_{bb'} - \tilde{\rho}_{b'b}) \quad (\text{A1c})$$

$$i \frac{\partial \tilde{\rho}_{cc}}{\partial t} = -\frac{\Omega_c}{2}(\tilde{\rho}_{c'c} - \tilde{\rho}_{cc'}) + \frac{\Omega_\mu}{2}(\tilde{\rho}_{ca} - \tilde{\rho}_{ac}) \quad (\text{A1d})$$

$$i \frac{\partial \tilde{\rho}_{c'c'}}{\partial t} = \frac{\Omega_c}{2}(\tilde{\rho}_{c'c} - \tilde{\rho}_{cc'}) \quad (\text{A1e})$$

and then the off-diagonals,

$$i \frac{\partial \tilde{\rho}_{ab}}{\partial t} = \Delta_p \tilde{\rho}_{ab} - \frac{\Omega_\mu}{2} \tilde{\rho}_{cb} + \frac{\Omega_b}{2} \tilde{\rho}_{ab'} + \frac{\Omega_p}{2}(\tilde{\rho}_{aa} - \tilde{\rho}_{bb}) \quad (\text{A1f})$$

$$i \frac{\partial \tilde{\rho}_{ab'}}{\partial t} = (\Delta_p - \Delta_b) \tilde{\rho}_{ab'} - \frac{\Omega_\mu}{2} \tilde{\rho}_{cb'} - \frac{\Omega_p}{2} \tilde{\rho}_{bb'} + \frac{\Omega_b}{2} \tilde{\rho}_{ab} \quad (\text{A1g})$$

$$i \frac{\partial \tilde{\rho}_{ca}}{\partial t} = -\Delta_\mu \tilde{\rho}_{ca} + \frac{\Omega_p}{2} \tilde{\rho}_{cb} - \frac{\Omega_\mu}{2}(\tilde{\rho}_{aa} - \tilde{\rho}_{cc}) - \frac{\Omega_c}{2} \tilde{\rho}_{c'a} \quad (\text{A1h})$$

$$i \frac{\partial \tilde{\rho}_{c'a}}{\partial t} = (\Delta_c - \Delta_\mu) \tilde{\rho}_{c'a} + \frac{\Omega_\mu}{2} \tilde{\rho}_{c'c} + \frac{\Omega_p}{2} \tilde{\rho}_{c'b} - \frac{\Omega_c}{2} \tilde{\rho}_{ca} \quad (\text{A1i})$$

$$i \frac{\partial \tilde{\rho}_{cb}}{\partial t} = (\Delta_p - \Delta_\mu) \tilde{\rho}_{cb} + \frac{\Omega_b}{2} \tilde{\rho}_{cb'} + \frac{\Omega_p}{2} \tilde{\rho}_{ca} - \frac{\Omega_\mu}{2} \tilde{\rho}_{ab} - \frac{\Omega_c}{2} \tilde{\rho}_{c'b} \quad (\text{A1j})$$

$$i\frac{\partial\tilde{\rho}_{cb'}}{\partial t} = (\Delta_p - \Delta_b - \Delta_\mu)\tilde{\rho}_{cb'} + \frac{\Omega_b}{2}\tilde{\rho}_{cb} - \frac{\Omega_\mu}{2}\tilde{\rho}_{ab'} - \frac{\Omega_c}{2}\tilde{\rho}_{c'b'} \quad (\text{A1k})$$

$$i\frac{\partial\tilde{\rho}_{c'b}}{\partial t} = (\Delta_p + \Delta_c - \Delta_\mu)\tilde{\rho}_{c'b} + \frac{\Omega_b}{2}\tilde{\rho}_{c'b'} + \frac{\Omega_p}{2}\tilde{\rho}_{c'a} - \frac{\Omega_c}{2}\tilde{\rho}_{cb} \quad (\text{A1l})$$

$$i\frac{\partial\tilde{\rho}_{c'b'}}{\partial t} = (\Delta_p - \Delta_b + \Delta_c - \Delta_\mu)\tilde{\rho}_{c'b'} + \frac{\Omega_b}{2}\tilde{\rho}_{c'b} - \frac{\Omega_c}{2}\tilde{\rho}_{cb'} \quad (\text{A1m})$$

$$i\frac{\partial\tilde{\rho}_{bb'}}{\partial t} = -\Delta_b\tilde{\rho}_{bb'} - \frac{\Omega_p}{2}\tilde{\rho}_{ab'} + \frac{\Omega_b}{2}(\tilde{\rho}_{bb} - \tilde{\rho}_{b'b'}) \quad (\text{A1n})$$

$$i\frac{\partial\tilde{\rho}_{c'c}}{\partial t} = \Delta_c\tilde{\rho}_{c'c} + \frac{\Omega_\mu}{2}\tilde{\rho}_{c'a} - \frac{\Omega_c}{2}(\tilde{\rho}_{cc} - \tilde{\rho}_{c'c'}) \quad (\text{A1o})$$

We have defined detunings $\Delta_p = \omega_a - \omega_b - \nu_p$, $\Delta_\mu = \omega_a - \omega_c - \nu_\mu$, $\Delta_b = \omega_{b'} - \omega_b - \nu_b$, and $\Delta_c = \omega_{c'} - \omega_c - \nu_c$.

APPENDIX B

We transform the equations of motion to first order in Ω_p/Ω_μ by diagonalizing the $\{|b\rangle, |b'\rangle\}$ and $\{|c\rangle, |c'\rangle\}$

subspaces of the Hamiltonian via the matrix

$$D = \begin{pmatrix} 1 & 0 & 0 & 0 & 0 \\ 0 & \cos\theta_b & \sin\theta_b & 0 & 0 \\ 0 & -\sin\theta_b & \cos\theta_b & 0 & 0 \\ 0 & 0 & 0 & \cos\theta_c & \sin\theta_c \\ 0 & 0 & 0 & -\sin\theta_c & \cos\theta_c \end{pmatrix} \quad (\text{B1})$$

where

$$\cos\theta_i = \sqrt{\frac{1 + \Delta_i/\Omega_i^{\text{eff}}}{2}} \quad \sin\theta_i = \sqrt{\frac{1 - \Delta_i/\Omega_i^{\text{eff}}}{2}}$$

and

$$\Omega_i^{\text{eff}} = \sqrt{\Delta_i^2 + \Omega_i^2}.$$

In this basis, the Hamiltonian becomes

$$D\tilde{\mathcal{H}}D^\dagger = \frac{\hbar}{2} \begin{pmatrix} 2\omega_a & -\Omega_p \cos\theta_b & \Omega_p \sin\theta_b & -\Omega_\mu \cos\theta_c & \Omega_\mu \sin\theta_c \\ -\Omega_p \cos\theta_b & 2\omega_b + \Delta_b + 2\nu_p - \Omega_b^{\text{eff}} & 0 & 0 & 0 \\ \Omega_p \sin\theta_b & 0 & 2\omega_b + \Delta_b + 2\nu_p + \Omega_b^{\text{eff}} & 0 & 0 \\ -\Omega_\mu \cos\theta_c & 0 & 0 & 2\omega_c + \Delta_c + 2\nu_\mu - \Omega_c^{\text{eff}} & 0 \\ \Omega_\mu \sin\theta_c & 0 & 0 & 0 & 2\omega_c + \Delta_c + 2\nu_\mu + \Omega_c^{\text{eff}} \end{pmatrix}. \quad (\text{B2})$$

Written, for now, without decay (which will require some approximations to transfer into this basis), we find

$$i\frac{\partial\tilde{\rho}_{aB}}{\partial t} = (\Delta_p - \frac{\Delta_b}{2} + \frac{\Omega_b^{\text{eff}}}{2})\tilde{\rho}_{aB} - \frac{\Omega_p}{2}(\cos\theta_b\tilde{\rho}_{BB} - \sin\theta_b\tilde{\rho}_{B'B}) - \frac{\Omega_\mu}{2}(\cos\theta_c\tilde{\rho}_{CB} - \sin\theta_c\tilde{\rho}_{C'B}) + \frac{\Omega_p}{2}\cos\theta_b\tilde{\rho}_{aa} \quad (\text{B3a})$$

$$i\frac{\partial\tilde{\rho}_{CB}}{\partial t} = (-\Delta_\mu + \Delta_p - \frac{\Delta_b}{2} + \frac{\Omega_b^{\text{eff}}}{2} + \frac{\Delta_c}{2} - \frac{\Omega_c^{\text{eff}}}{2})\tilde{\rho}_{CB} + \frac{\Omega_p}{2}\cos\theta_b\tilde{\rho}_{Ca} - \frac{\Omega_\mu}{2}\cos\theta_c\tilde{\rho}_{aB} \quad (\text{B3b})$$

$$i\frac{\partial\tilde{\rho}_{C'B}}{\partial t} = (-\Delta_\mu + \Delta_p - \frac{\Delta_b}{2} + \frac{\Omega_b^{\text{eff}}}{2} + \frac{\Delta_c}{2} + \frac{\Omega_c^{\text{eff}}}{2})\tilde{\rho}_{C'B} + \frac{\Omega_p}{2}\cos\theta_b\tilde{\rho}_{C'a} + \frac{\Omega_\mu}{2}\sin\theta_c\tilde{\rho}_{aB} \quad (\text{B3c})$$

and

$$i\frac{\partial\tilde{\rho}_{aB'}}{\partial t} = (\Delta_p - \frac{\Delta_b}{2} - \frac{\Omega_b^{\text{eff}}}{2})\tilde{\rho}_{aB'} - \frac{\Omega_p}{2}(\cos\theta_b\tilde{\rho}_{BB'} - \sin\theta_b\tilde{\rho}_{B'B'}) - \frac{\Omega_\mu}{2}(\cos\theta_c\tilde{\rho}_{CB'} - \sin\theta_c\tilde{\rho}_{C'B'}) - \frac{\Omega_p}{2}\sin\theta_b\tilde{\rho}_{aa} \quad (\text{B4a})$$

$$i\frac{\partial\tilde{\rho}_{CB'}}{\partial t} = (-\Delta_\mu + \Delta_p - \frac{\Delta_b}{2} - \frac{\Omega_b^{\text{eff}}}{2} + \frac{\Delta_c}{2} - \frac{\Omega_c^{\text{eff}}}{2})\tilde{\rho}_{CB'} - \frac{\Omega_p}{2}\sin\theta_b\tilde{\rho}_{Ca} - \frac{\Omega_\mu}{2}\cos\theta_c\tilde{\rho}_{aB'} \quad (\text{B4b})$$

$$i\frac{\partial\tilde{\rho}_{C'B'}}{\partial t} = (-\Delta_\mu + \Delta_p - \frac{\Delta_b}{2} - \frac{\Omega_b^{\text{eff}}}{2} + \frac{\Delta_c}{2} + \frac{\Omega_c^{\text{eff}}}{2})\tilde{\rho}_{C'B'} - \frac{\Omega_p}{2}\sin\theta_b\tilde{\rho}_{C'a} + \frac{\Omega_\mu}{2}\sin\theta_c\tilde{\rho}_{aB'} \quad (\text{B4c})$$

In this partially diagonalized basis, we have $\tilde{\rho}_{ab} = \cos\theta_b\tilde{\rho}_{aB} - \sin\theta_b\tilde{\rho}_{aB'}$, $\tilde{\rho}_{Ca} = \cos\theta_c\tilde{\rho}_{Ca} + \sin\theta_c\tilde{\rho}_{C'a}$, and $\tilde{\rho}_{C'a} = \cos\theta_c\tilde{\rho}_{C'a} - \sin\theta_c\tilde{\rho}_{Ca}$. Meanwhile,

$$\begin{pmatrix} \tilde{\rho}_{BB} & \tilde{\rho}_{BB'} \\ \tilde{\rho}_{B'B} & \tilde{\rho}_{B'B'} \end{pmatrix} = \begin{pmatrix} \cos^2\theta_b\tilde{\rho}_{bb} + \cos\theta_b\sin\theta_b(\tilde{\rho}_{b'b} + \tilde{\rho}_{bb'}) & \sin^2\theta_b\tilde{\rho}_{b'b'} & \sin\theta_b\cos\theta_b(\tilde{\rho}_{b'b'} - \tilde{\rho}_{bb}) + \cos^2\theta_b\tilde{\rho}_{bb'} - \sin^2\theta_b\tilde{\rho}_{b'b} \\ \sin\theta_b\cos\theta_b(\tilde{\rho}_{b'b'} - \tilde{\rho}_{bb}) + \cos^2\theta_b\tilde{\rho}_{b'b} - \sin^2\theta_b\tilde{\rho}_{bb'} & \cos^2\theta_b\tilde{\rho}_{b'b'} - \cos\theta_b\sin\theta_b(\tilde{\rho}_{b'b} + \tilde{\rho}_{bb'}) & \sin^2\theta_b\tilde{\rho}_{bb} \end{pmatrix}.$$

APPENDIX C

To incorporate decay in the dressed basis, we have to make certain assumptions, as described in the text. These amount to saying that $\gamma_{ab} \approx \gamma_{ab'}$ and that $\gamma_b \approx \gamma_{b'}$, $\gamma_{bc}^{\text{ph}} \approx \gamma_{b'c}^{\text{ph}}$, and $\gamma_{bc'}^{\text{ph}} \approx \gamma_{b'c'}^{\text{ph}}$ so that we can take $\gamma_{cb} \approx \gamma_{cb'} = \gamma_C$ and $\gamma_{c'b} \approx \gamma_{c'b'} = \gamma_{C'}$. Under these approximations, the contributions from decay and dephasing are

$$i\dot{\tilde{\rho}}_{aB} \sim -i\gamma_{ab}\tilde{\rho}_{aB} \quad (\text{C1a})$$

$$i\dot{\tilde{\rho}}_{aB'} \sim -i\gamma_{ab}\tilde{\rho}_{aB'} \quad (\text{C1b})$$

$$i\dot{\tilde{\rho}}_{CB} \sim -i(\gamma_C \cos^2 \theta_c + \gamma_{C'} \sin^2 \theta_c)\tilde{\rho}_{CB} \\ - i(\gamma_{C'} - \gamma_C) \cos \theta_c \sin \theta_c \tilde{\rho}_{CB} \quad (\text{C1c})$$

$$i\dot{\tilde{\rho}}_{C'B} \sim -i(\gamma_C \sin^2 \theta_c + \gamma_{C'} \cos^2 \theta_c)\tilde{\rho}_{C'B} \\ - i(\gamma_{C'} - \gamma_C) \cos \theta_c \sin \theta_c \tilde{\rho}_{C'B} \quad (\text{C1d})$$

$$i\dot{\tilde{\rho}}_{CB'} \sim -i(\gamma_C \cos^2 \theta_c + \gamma_{C'} \sin^2 \theta_c)\tilde{\rho}_{CB'} \\ - i(\gamma_{C'} - \gamma_C) \cos \theta_c \sin \theta_c \tilde{\rho}_{CB'} \quad (\text{C1e})$$

$$i\dot{\tilde{\rho}}_{C'B'} \sim -i(\gamma_C \sin^2 \theta_c + \gamma_{C'} \cos^2 \theta_c)\tilde{\rho}_{C'B'} \\ - i(\gamma_{C'} - \gamma_C) \cos \theta_c \sin \theta_c \tilde{\rho}_{C'B'} \quad (\text{C1f})$$

For completeness, we present here a complete and general solution for the reduced susceptibility, $\tilde{\chi}^{(1)}$, including arbitrary detunings of all fields. We find

$$\tilde{\chi}^{(1)} = \frac{2\gamma_{ab}}{\Omega_p} (\cos \theta_b \tilde{\rho}_{aB} - \sin \theta_b \tilde{\rho}_{aB'}). \quad (\text{D1})$$

Here,

$$\tilde{\rho}_{aB} = \frac{\Omega_p}{Z_+} ((\sin \theta_b \tilde{\rho}_{B'B} - \cos \theta_b \tilde{\rho}_{BB}) (- (2i\gamma_C + \Delta_b - \Delta_c - 2\delta - \Omega_b^{\text{eff}}) (2i\gamma_{C'} + \Delta_b - \Delta_c - 2\delta - \Omega_b^{\text{eff}}) \\ + 2i \cos(2\theta_c) (\gamma_C - \gamma_{C'}) \Omega_c^{\text{eff}} + (\Omega_c^{\text{eff}})^2) + \cos \theta_b \cos \theta_c \tilde{\rho}_{Ca} (2i\gamma_{C'} + \Delta_b - \Delta_c - 2\delta - \Omega_b^{\text{eff}} - \Omega_c^{\text{eff}}) \Omega_\mu \\ - \cos \theta_b \sin \theta_c \tilde{\rho}_{C'a} (2i\gamma_{C'} + \Delta_b - \Delta_c - 2\delta - \Omega_b^{\text{eff}} + \Omega_c^{\text{eff}}) \Omega_\mu) \quad (\text{D2})$$

and

$$\tilde{\rho}_{aB'} = \frac{\Omega_p}{Z_-} ((\sin \theta_b \tilde{\rho}_{B'B'} + \cos \theta_b \tilde{\rho}_{BB'}) (- (2i\gamma_C + \Delta_b - \Delta_c - 2\delta + \Omega_b^{\text{eff}}) (2i\gamma_{C'} + \Delta_b - \Delta_c - \delta + \Omega_b^{\text{eff}}) \\ + 2i \cos(2\theta_c) (\gamma_C - \gamma_{C'}) \Omega_c^{\text{eff}} + (\Omega_c^{\text{eff}})^2) - \sin \theta_b \cos \theta_c \tilde{\rho}_{Ca} (2i\gamma_{C'} + \Delta_b - \Delta_c - 2\delta + \Omega_b^{\text{eff}} - \Omega_c^{\text{eff}}) \Omega_\mu \\ + \sin \theta_b \sin \theta_c \tilde{\rho}_{C'a} (2i\gamma_{C'} + \Delta_b - \Delta_c - 2\delta + \Omega_b^{\text{eff}} + \Omega_c^{\text{eff}}) \Omega_\mu) \quad (\text{D3})$$

where now

$$Z_\pm = \sin^2 \theta_c (2i\gamma_{C'} + \Delta_b - \Delta_c - 2\delta \mp \Omega_b^{\text{eff}} + \Omega_c^{\text{eff}}) \Omega_\mu^2 + 2i \cos^2 \theta_c \sin^2 \theta_c (\gamma_C - \gamma_{C'}) (2i(\gamma_C - \gamma_{C'}) \\ \times (2\gamma_{ab} + \Delta_b - 2\Delta_p \mp \Omega_b^{\text{eff}}) - \Omega_\mu^2) + (-2i \sin^2 \theta_c \gamma_C - 2i \cos^2 \theta_c \gamma_{C'} - \Delta_b + \Delta_c + 2\delta \pm \Omega_b^{\text{eff}} + \Omega_c^{\text{eff}}) \\ \times ((2i\gamma_{ab} + \Delta_b - 2\Delta_p \mp \Omega_b^{\text{eff}}) (2i \cos^2 \theta_c \gamma_C + 2i \sin^2 \theta_c \gamma_{C'} + \Delta_b - \Delta_c - 2\delta \mp \Omega_b^{\text{eff}} + \Omega_c^{\text{eff}}) - \cos^2 \theta_c \Omega_\mu^2). \quad (\text{D4})$$

We have defined the two photon detuning, $\delta = \Delta_p - \Delta_\mu = \omega_c - \omega_b + \nu_\mu - \nu_p$.

In the special case that $\cos \theta_b \tilde{\rho}_{BB} - \sin \theta_b \tilde{\rho}_{B'B} = \sin \theta_b \tilde{\rho}_{B'B'} + \cos \theta_b \tilde{\rho}_{BB'}$, we can define $\mathfrak{P}_B = \sqrt{2}(\cos \theta_b \tilde{\rho}_{BB} - \sin \theta_b \tilde{\rho}_{B'B})$. Likewise, when $\sin \theta_c \tilde{\rho}_{Ca} = \cos \theta_c \tilde{\rho}_{C'a}$, we can define $\mathfrak{P}_C = -\frac{2\Omega_\mu}{\Omega_c^{\text{eff}}} \sin \theta_c \tilde{\rho}_{Ca}$. Then Eqs. D2 and D3 take on the relatively simple form familiar from the body of the paper,

$$\tilde{\rho}_{aB} = \frac{\Omega_p}{Z_+} (\mathfrak{P}_B ((2i\gamma_C + \Delta_b - \Delta_c - 2\delta - \Omega_b^{\text{eff}}) (2i\gamma_{C'} + \Delta_b - \Delta_c - 2\delta - \Omega_b^{\text{eff}}) - 2i \cos(2\theta_c) (\gamma_C - \gamma_{C'}) \Omega_c^{\text{eff}}) \\ + (\Omega_c^{\text{eff}})^2 (\cos \theta_b \mathfrak{P}_C - \mathfrak{P}_B)) \quad (\text{D5})$$

and

$$\tilde{\rho}_{aB'} = -\frac{\Omega_p}{Z_-} (\mathfrak{P}_B ((2i\gamma_C + \Delta_b - \Delta_c - 2\delta + \Omega_b^{\text{eff}}) (2i\gamma_{C'} + \Delta_b - \Delta_c - \delta + \Omega_b^{\text{eff}}) - 2i \cos(2\theta_c) (\gamma_C - \gamma_{C'}) \Omega_c^{\text{eff}}) \\ + (\Omega_c^{\text{eff}})^2 (\sin \theta_b \mathfrak{P}_C - \mathfrak{P}_B)). \quad (\text{D6})$$

-
- [1] Lord Rayleigh, *Phil. Mag. & Jour. of Sci.* **XLVIII**, 151 (1899).
- [2] L. Brillouin, *Wave propagation and group velocity* (Academic Press, New York, 1960).
- [3] C. G. B. Garrett and D. E. McCumber, *Phys. Rev. A* **1**, 305 (1970).
- [4] G. Diener, *Physics Letters A* **223** (1996).
- [5] B. Macke and B. Ségard, *Euro. Phys. J. D* **23**, 125 (2003).
- [6] A. Kuzmich, A. Dogariu, L. J. Wang, P. W. Milonni, and R. Y. Chiao, *Phys. Rev. Letters* **86**, 3925 (2001).
- [7] C.-G. Huang and Y.-Z. Zhang, *Phys. Rev. A* **65**, 015802 (2001).
- [8] L. J. Wang, A. Kuzmich, and A. Dogariu, *Nature* **406**, 277 (2000).
- [9] A. Kuzmich, A. Dogariu, and L. J. Wang, *Phys. Rev. A* **63**, 053806 (2001).
- [10] A. M. Steinberg and R. Y. Chiao, *Phys. Rev. A* **49**, 2071 (1994).
- [11] M. S. Bigelow, N. N. Lepeshkin, and R. W. Boyd, *Science* **301**, 200 (2003).
- [12] M. S. Bigelow, N. N. Lepeshkin, and R. W. Boyd, *J. Phys.: Cond. Mat.* **16**, 1321 (2004).
- [13] M. D. Stenner, D. J. Gauthier, and M. A. Neifeld, *Nature* **425**, 695 (2003).
- [14] A. D. Wilson-Gordon and H. Friedmann, *Opt. Comm.* **94**, 238 (1992).
- [15] C. Szymanowski and C. Keitel, *J. Phys. B* **27**, 5795 (1994).
- [16] T. Quang and H. Freedhoff, *Phys. Rev. A* **48**, 3216 (1993).
- [17] A. Wicht, K. Danzmann, M. Fleischhauer, M. Scully, G. Muller, and R.-H. Rinkleff, *Opt. Comm.* **134**, 431 (1997).
- [18] A. Rocco, A. Wicht, R.-H. Rinkleff, and K. Danzmann, *Phys. Rev. A* **66**, 053804 (2002).
- [19] H. Friedmann and A. D. Wilson-Gordon, *Opt. Comm.* **98**, 303 (1993).
- [20] A. Rosenhouse-Dantsker, A. D. Wilson-Gordon, and H. Friedmann, *Opt. Comm.* **113**, 226 (1994).
- [21] A. Wicht, R.-H. Rinkleff, L. S. Molella, and K. Danzmann, *Phys. Rev. A* **66**, 063815 (2002).
- [22] D. Bortman-Arbiv, A. D. Wilson-Gordon, and H. Friedmann, *Phys. Rev. A* **63**, 043818 (2001).
- [23] G. S. Agarwal, T. N. Dey, and S. Menon, *Phys. Rev. A* **64**, 053809 (2001).
- [24] R. G. Ghulghazaryan and Y. P. Malakyan, *Phys. Rev. A* **67**, 063806 (2003).
- [25] C. Goren, A. D. Wilson-Gordon, M. Rosenbluh, and H. Friedmann, *Phys. Rev. A* **68**, 043818 (2003).
- [26] H. Kang, L. Wen, and Y. Zhu, *Phys. Rev. A* **68**, 063806 (2003).
- [27] H. Kang, G. Hernandez, and Y. Zhu, *Phys. Rev. A* **70**, 011801(R) (2004).
- [28] G. S. Agarwal and S. Dasgupta, *Phys. Rev. A* **70**, 023802 (2004).
- [29] X. ming Hu, G. ling Cheng, J. hua Zou, X. Li, and D. Du, *Phys. Rev. A* **72**, 023803 (2005).
- [30] Q.-F. Chen, Y.-S. Zhang, B.-S. Shi, and G.-C. Guo, *Phys. Rev. A* **78**, 013804 (2008).
- [31] H. Tajalli and M. Sahrari, *J. Opt. B* **7**, 168 (2005).
- [32] M. Sahrari, H. Tajalli, K. T. Kapale, and M. S. Zubairy, *Phys. Rev. A* **70**, 023813 (2004).
- [33] L.-G. Wang, S. Qamar, S.-Y. Zhu, and M. S. Zubairy, *Phys. Rev. A* **77**, 033833 (2008).
- [34] J. O. Weatherall and C. P. Search, *Phys. Rev. A* **78**, 053802 (2008).
- [35] J. O. Weatherall, C. P. Search, and M. Jääskeläinen, *Phys. Rev. A* **78**, 013830 (2008).
- [36] M. D. Lukin, S. F. Yelin, M. Fleischhauer, and M. O. Scully, *Phys. Rev. A* **60**, 3225 (1999).
- [37] M. Yan, E. G. Rickey, and Y. Zhu, *Phys. Rev. A* **64**, 013412 (2001).
- [38] S. F. Yelin, V. A. Sautenkov, M. M. Kash, G. R. Welch, and M. D. Lukin, *Phys. Rev. A* **68**, 063801 (2003).
- [39] C. Y. Ye, A. S. Zibrov, Y. V. Rostovtsev, and M. O. Scully, *Phys. Rev. A* **65**, 043805 (2002).
- [40] M. Mahmoudi, R. Fleischhaker, M. Sahrari, and J. Evers, *J. Phys. B: At. Mol. Opt. Phys.* **41**, 025504 (2008).
- [41] Y.-C. Chen, Y.-A. Liao, H.-Y. Chiu, J.-J. Su, and I. A. Yu, *Phys. Rev. A* **64**, 053806 (2001).
- [42] E. A. Wilson, N. B. Manson, and C. Wei, *Phys. Rev. A* **72**, 063814 (2005).
- [43] M. M. Kash, V. A. Sautenkov, A. S. Zibrov, L. Holberg, G. R. Welch, M. D. Lukin, Y. Rostovtsev, E. S. Fry, and M. O. Scully, *Phys. Rev. Lett.* **82**, 5229 (1999).
- [44] K. Kim, H. S. Moon, C. Lee, S. K. Kim, and J. B. Kim, *Phys. Rev. A* **68**, 013810 (2003).
- [45] O. Kocharovskaya, *Phys. Rep.* **219**, 175 (1992).
- [46] J. Mompert and R. Corbalaán, *J. Opt. B* **2**, 7 (2000).
- [47] M. O. Scully and M. S. Zubairy, *Quantum Optics* (Cambridge University Press, Cambridge, 1997).
- [48] O. Kocharovskaya and Y. I. Khanin, *Sov. Phys. JETP Lett.* **48**, 630 (1988).
- [49] S. E. Harris, *Phys. Rev. Lett.* **62**, 1033 (1989).
- [50] L. V. Hau, S. E. Harris, Z. Dutton, and C. H. Behroozi, *Nature* **397**, 594 (1999).
- [51] D. Budker, D. F. Kimball, S. M. Rochester, and V. V. Yashchuk, *Phys. Rev. Lett.* **83**, 1767 (1999).